SAPIENZA
UNIVERSITÀ DI ROMA

Development of a new device for the measurement and modeling of an innovative Risk Index for Cultural Heritage application

Faculty of Civil and Industrial Engineering

Department of Mechanical and Aerospace Engineering

Industrial and Management Engineering – XXXI cycle

Supervisors

Prof. Paolo Cappa

Prof. Zaccaria Del Prete

Ph.D. Candidate

Livio D'Alvia

Academic Year. 2018-2019

To Prof. Cappa

Part 1: Background

This section contains a brief general survey about the air quality monitoring and a more specific survey on Cultural Heritage.

The monitoring, as a function of time, of environmental parameters in cultural heritage is essential to preserve materials, to recognize the reasons of degradation and to evaluate their effects.

The degrading effects of objects in cultural heritage field, can be classified in optical, morphological, physical-chemical/mechanical and alterations and depend by micro-climatic conditions. For this reason, in recent years, several solutions have been developed and commercialized for environmental monitoring, some compatible with general advice and others OEM (Original Equipment Manufacturing). However, the trend of application between compliant and non-ISO-compliant devices has not yet been sufficiently analyzed.

In this first section, we show how in the last ten years researchers have shifted their attention to custom-made devices based on new generation sensors despite the expense of units ISO certified.

The study based on a review of scientific articles has shown that: with the increase of low-cost and open-source technologies applied in the Environmental Impact Assessment (EIA) and in particular in the cultural heritage, led to a research advancement in the field, but, at the same time, increased non-homogeneity of the methods, impinging comparability of results.

In recent years the trend is to use low-cost automatic wireless systems. This innovation, however, opens new scenarios and challenges on how to improve their stability, longevity and sensitivity; reduce maintenance (battery replacement, including calibration or sensors); improve data analysis/management/display costs. In particular, it has highlighted the current difficulty of low-cost detectors to satisfy the robustness and reliability of regulatory and conventional stationary monitors at the expense of the

periods and aesthetics. We have therefore paid particular attention to the sensitivity and reliability of the innovative solutions presented to overcome the traditional limitations, as well as to the real feasibility of solutions regarding sustainability, adaptability to the works of art or price. We also see the need for more communication between the scientific community and the decision-makers, who have only recently opened up to this paradigm. We highlighted the need to identify recurrent or innovative topics in the various documents concerning the approaches to preventive conservation, the preservation of damage and environmental management.

The literature review reported in this section will settle the basis of the research work described in sections 2 and 3.

INTRODUCTION

In the last years, the interest of the Scientific Community in environmental monitoring has considerably increased [1], [2] due to the smog that may result in widely impacts, causing diverse effects on the environment, on human health, or the economy of developing and industrialized countries. Accordingly to these, air quality assessment is commonly required by health and environmental regulations that are both international and national, to evaluate the environmental exposure systematically [3]. The equipment used to collect pollutants and following the international standard, by environmental or government authorities are based on a network of fixed monitoring stations instrumented with certified and specialized devices for measuring multiple environmental contaminants.

Studies in which authors apply low-cost sensors were also carried out by researchers [4]–[6], showing how nowadays, it is possible to collect the environmental information by sparse and miniaturized low-cost platforms applied in a wide range of purposes and contests (such as healthcare, manufacturing, conservation) and manufactured with nonhomogeneous technologies.

In both cases, the platforms are generally equipped with devices able to measure regulatory pollutants such as nitrogen oxides (NO, NO_2, NO_x), carbon monoxide (CO), sulfur dioxide (SO_2), ozone (O_3) and particulate matter (PM_{10}, $PM_{2.5}$) [7].

The substantial difference between the traditional fixed-site stations and the other kind of platforms is that the first class of instruments must comply with EU Air Quality Directive (AQD) [8] which establishes the standard criteria for air quality monitoring, as well as defining the reference measurement methods and

the standard procedure methods for instrument data collection, post-processing and calibration..

Usually, air pollutant/air quality monitoring is performed using analytical instruments, such as chemical and optical analyzers, that are bulky, cumbersome and expensive with prices ranging between 10000 € and 90000 € per single devices or combined solution[1]. For instance, the investment and installation of single gas sampler could cost between 10000 € and 15000 € while the integration of particulate sampler in an existing station could cost between 10000 € to 30000 €. Ultimately, a multipollutant analyzer could cost 50000 € - 90000 € [2].

Moreover, a significant amount of resources must be added to the price for the routine procedures required to maintain and calibrate them and also to guarantee comparability and high-quality data between different stations and nations. At last to the economic problem, traditional air quality stations are located at strategic fixed-site areas and can provide accurate data only for a restricted area [9]

A current trend, in the research area, explores the possibility to use economic sensors and devices in complementarity or substitution of the traditional ones and it is supported by the report EU AQD report no. 28 [10] that provides the opportunity to do not use certified sensors to acquire indicative measurements in support of objective estimation for air quality assessment, as long as they comply with the quality objectives set for each pollutant [11].

In particular, the devices able to detect the pollutant concentrations could be classified in i) sensors that measure the interaction between the pollutant and sensing material (i.e., metal-oxide sensors or electrochemical sensors), or ii) sensors that measure the light scattering or the absorption of light (infrared and

[1] The prices of instrumentations are averaged to the confidential invoices provided by different producers

visible range). Nowadays new kind of sensors has been added to these technologies, in particular, micro-electro-mechanical systems or MEMS.

Another advantage of a not-regulatory solution consists of integrating into a single board only sensors able to detect the concentrations of air pollutant for a selected and specific subject; this method can be used both indoors and outdoors. Nevertheless, the price of single sensors is from 15 € to 150 € while the cost of a customized sensor node can reach[2] 500 € – 5000 €.

Moreover, these devices are commonly accomplished with an advanced microcomputer for data manipulation, elaboration and visualization [4], [12].

The easy to use and compactness characteristic, the high spatial and temporal resolution [13], as well as the continuous real-time measurement of smog, are the reasons for increasingly widespread using [14].

Under this hypothesis, the application of spread miniaturized low-cost devices/sensors becomes useful in a particular application as the monitoring in Cultural Heritage field, where non-aesthetic fixed control units near to a monument or artefact are to be avoided.

For this reason, a state of the art of the sensors applied in the Cultural Heritage will be proposed focusing on the last ten years trends in small, portable gaseous air pollution monitor use and the technologies evolution. Also, answers will be given to two open questions and challenges will be faced regarding their application that could be summarized as follow: a) Is there a real exigency for applying low-cost air pollution detectors in an archaeological site? b) Do these low-cost solutions guarantee sensitivity, selectivity and robustness enough for reliable long-term performance?

Furthermore, an overview of the effect of the air pollution Cultural Heritage is anticipated and focused on the selected parameters into this dissertation.

[2] The prices of sensors are averaged to the confidential invoices provided by different producers

State of Art

Monitoring is an activity required a both after-damage and preventive risk assessment. Different tools for the monitoring activities make available different previsions, such as episodic and/or continuous, short-term and/or long-term, or qualitative and/or quantitative. For these reasons, a literature review was conducted using the results of 3 different databases (Google Scholar, Scopus and ISI Web of Knowledge). The electronic search was performed using the combinations of the following keywords: WSN, Cultural Heritage, Monitoring Device, Air Quality. For each database, we used the same words list and their combinations. Both query structure and the keywords were arranged as a function of the writing rules required by the selected database. The electronic search of the previously mentioned database identifies 150 published studies. After a process of screening based on inclusion criteria (only scientific papers, published until 2009, written in the English language, keywords and abstract coherence) and exclusion criteria (conference proceedings were not reported), only 24 papers were considered in the present review.

The other two parameters such as dimension and cost are taken marginally in the discussion due to the arbitrariness of the definition of small-size, the lack of development of instruments from universities and the unavailability of prices.

We decided to analyze the applied technologies classifying pollution monitoring instruments into four categories: direct application of active sampling, indirect application of active sampling (such as a mathematical interpolation model of national air monitoring networks data), passive sampling and, at last, sensor-based devices [15], [16].

Direct active sampling devices

This kind of device is principally manufactured for governmental environmental monitoring. They are large and sophisticated instruments (even >

20 kg) [17], which measure pollutants (single or not), with a sensitivity higher than it is needed in the cultural heritage field. They are based on chemiluminescence and/or fluorescence proprieties where the targeted pollutant absorbs radiation or reacts with a chemical compound, leading to the emission of light as a consequence, which can then be detected and analyzed. However, the costs and the complexities of active sampling analyzers limit their application in an ordinary survey.

For example Saraga et al. [18] discussed the application of measurement units for external environmental monitoring, including: (i) ultraviolet photometry automatic analyzers for O_3 (EN 14625:05); (ii) ultraviolet fluorescence for SO_2 (EN 14212:05); (iii) chemiluminescence for NO_x (EN 14211:05) and (iv) gravimetric measurement for PM_{10} (EN 12341:99) and $PM_{2.5}$ (EN 14907:05). The proposed instrumentation generally has a dimension of 42.5 cm (W), 157.5 cm (H), 58.5 cm (D), occupying a volume that could be incompatible with heritage applications and having a price of 10.000 €.

Indirect active sampling devices

Recent studies show a no-cost solution: the possibility to use, when accessible, pollution data acquired from a nearby national monitoring station networks and to evaluate pollution levels using mathematical models [19]. Under this hypothesis De la Fuente et al. [20], [21] and Karaka et al. [22] evaluated a model to identify the corrosion rate of cultural heritage materials, correlating spares monitoring stations and analyzing the effect of different pollutants. Screpanti [23], [24] et al., focused their attention on both Italy and Europe using the data obtained by all Italian environmental institutions (local ARPA website) and international institution. A limitation of this technique regards the different empirical formulas provided by single authors [25].

Passive devices and Dosimeters

Passive sampling devices and dosimeters react to the presence of pollutants with observable changes in their optical/physical properties (for example corrosion or color alteration) and a qualitative measure is provided.

For example, Maskova et al. [26], Grontoft et al. [27], Worobeic et al. [28], evaluated the concentrations of NO_2, SO_2, O_3, acetic and formic acids, HNO_3 and NH_3 indoors and outdoors at five different archives.

Due to their properties, they have been used to realize dosimeters for a wide range of pollutants and have been used in cultural heritage for "for a very long time environmental monitoring. Currently, they are being replaced due to the difficulty of being integrated into a compact autonomous unit and because of the cumulative response to the synergistic effects of environmental parameters that require a post-acquiring analysis (Gas or Ion Chromatography, SEM), they are causing an increase of the final cost. In their research, Carminati et al. [29] proposed pocket-sized personal dosimeters applicable on a digital camera. This solution could open the possibility to integrate a dosimeter device into the sensors based devices described above.

Sensor-based devices

The development of low-cost environmental monitoring methods has encouraged the creation of a wide number of commercially available air quality sensors and prototype sensor networks. Currently, three detection methods for pollutants exist: electrochemical, photometric and microelectromechanical (MEMS) sensors. This technology enables the integration in a small-scale, sensor-arrays solution in order to measure different pollutant compounds. Even if the technology is still in development, it presents more valuable pros as the ability to measure small pollutant concentrations such as ozone, nitrogen oxides and sulfur dioxide, typically lower then twenty ppb.

Despite an end-user perspective of low-cost sensors for outdoor air pollution monitoring, this technology finds a broad application principally in the indoor application as shown in many research [30]–[35]. All authors highlighted the importance of investigating the fluctuation of air temperature (T) and percentage relative humidity (%RH), identifying these parameters as a determinant in the deterioration of collected artifacts. At the same time, they pointed out the difficulty to install sparse measurement stations preserving artworks appearance.

In recent year [36]–[40] some authors highlight the needs of methodologies to sample the Inorganic or Volatile Organic Compounds (NO_x, O_3, SO_x, VOC) and particulate matter. In these studies, however, the evaluation of gaseous compound is marginally compared to the analysis of Temperature or Moister level.

At the current stage, low-cost, small-scale solutions, as proposed by Mead *et al.* [41] that show the real benefits related to low-cost sensing are limited only in the generic or environmental health monitoring. It is far to be applied in cultural heritage field [42] a solution that integrated in a single board: (i) an environmental parameter sensor (temperature, relative humidity, barometric pressure); (ii) an electrochemical cell to monitor gas pollutant; (iii) one optical particle counter (OPC) to control the total particle matter; and (iv) an anemometer to analyze the wind direction and intensity.

Spinelle et al. [43], [44] The sensor-based devices, contrariwise permit to monitor a chosen monument or museum's room locally highlighted the sensitivity and accuracy of low-cost sensor devices applied to environmental monitoring. In particular, they show how the evaluated accuracy for O_3, NO_2, NO, CO and CO_2 reach the just cited Data Quality Objective (DQOs) of the European Air Quality Directive [8].

About the real exigency for applying low-cost air pollution detectors in an archeological site/museum, the proposed review shows how the application of: (i) direct active sampler is limited to spot pollution monitoring; (ii) indirect active systems provide an empirical interpretation of the corrosion rate analyzing a wide area (whole city or region) and not the environment around a specific monument; (iii) passive systems, independently to low cost, haven't got a proper selectivity of pollutants. Contrariwise a wireless sensor network allows monitoring a chosen monument or museum's room locally. Moreover, many proposed studies highlight how low-cost solutions guarantee sensitivity and selectivity for long-term performance.

For this reason, we decide to realize a prototype able to detect not only temperature and relative humidity fluctuation but the concentration of gaseous pollutant and structural vibration as primary output.

In the following subsection, environmental parameters and their effects are discussed.

Table 1 Summary of sampling characteristics

Reference	Pollutant	type	Measuring	Sensitivity	cost[a]
Saraga et al. [18]	O_3, SO_2, NO_2 and PM_{TOT}	Direct Active sampling devices	Instantaneous pollutant concentrations	Fraction of ppb	€€€€
Hamilton et al. [19]	O_3, SO_2, NO_2 and PM_{TOT}	Indirect Active sampling devices	Mathematical model	Erosion rate	free
De la Fuente et al. [20], [21]	O_3, SO_2, NO_2 and PM_{TOT}	Indirect Active sampling devices	Mathematical model	Erosion rate	free
Karaca [22]	NO_2 O_3, SO_2	Indirect Active sampling devices	Mathematical model	Erosion rate	free
Screpanti et al. [23], [24]	O_3, SO_2, NO_2 and PM_{TOT}	Indirect Active sampling devices	Mathematical model	Erosion rate	free
Maskova et al. [26]	O_3, SO_2, NO_2 acetic and formic acids, HNO3 and NH3	Single-use dosimeters	Averaged dose	Typically depends on size and thickness	€
Grotntoft et al. [27]	O_3, SO_2, NO_2, acetic and formic acids, HNO3 and NH3	Single-use dosimeters	Averaged dose	Typically depends on size and thickness	€
Worobeic wt al.		Sensor-based devices	Instantaneous concentrations	n/a	€
Carminati et al. [29]	$PM_{2.5}$	Research prototypes	Averaged dose	n/a	n/a
Sciurpi et al. [30]	T and %RH	Sensor-based devices	Instantaneous concentrations	: ±0.5 ◦C ± 2%	n/a
Grygierek et al. [31], [34], [35]	T, %RH and SO_2	Sensor-based devices	Instantaneous concentrations	± 1.8 °C ± 3% ±40 ppm	€€€
Krupinska et al. [36], [37]	T, %RH, NO2, SO2, O3 and particulate matter	Sensor-based devices	Averaged dose	n/a	n/a
Godoi et al. [38]	T, %RH, O_3, SO_2, NO_2, acetic and formic acids, HNO3 and NH3	Sensor-based devices Single-use dosimeters	Averaged dose	n/a	n/a
Lamonaca et al. [39]	T, %RH	Sensor-based devices	Instantaneous concentrations	n/a	€€

[a]€ cheap, €€ quite expensive, €€€ expensive, €€€€ very expensive, n/a not available.

Environmental parameters and Effects

The causes of degradation are generally localized in the environment around the monument, for this reason, is possible to talk about Environmental Impact [45]. The environment has always tallied a vital role in the life-cycle of an artwork/monument, due to interaction with the materials. However, the development of industrial society and especially around the second half of the last century has produced a profound change that has drastically accelerated the degradation of cultural heritage materials [46].

Different authors, as Tidball et al. and Watt et al. [47], [48], described the degradation of materials due to atmospheric action. They point out it as responsible of the severe decline of air quality due to the copious gaseous emissions of anthropogenic activities that have introduced new agents in the environment, many of them hazardous for cultural heritage conservation [49]. Two of these, in the form of gases, nitrogen oxides NO_x and sulfur dioxide SO_2 are the precursors of strong acids, respectively nitric acid (HNO_3) and sulfuric acid (H_2SO_4), extremely aggressive for the carbonate materials such as marble, limestone – widely applied in ancient architecture – and the plaster. Moreover, as widely demonstrated in the literature [50]–[54], this pollutant represent a risk for the carbonatic-based artworks due to the direct interaction between the pollutants, gaseous or in the shape of acid rains and the underlying stone layer. Gypsum is the result of this process. It can absorb and include many black carbon particles producing the so-called "black crust," and it is responsible to the dissolution and deterioration of statues or frescos [49].

At the same time, the airborne particulate is based on coal and oil. The first one carries out a high disfiguring action, in particular, when it settles and accumulates on statues, facades, monuments, due to the black color, while the

second (demi-combust oils or other hydrocarbons) are greasy and sticky, still adhere to the surface and allow permanent attachment of other particles.

Furthermore, there are physical factors such as temperature and humidity. The danger, in this case, is not so much in the absolute values but in the fluctuations of these parameters, which generate degrading stresses in almost all the materials. Related to the humidity, the condensation conveys salts and gases in solution, accelerating the interaction with the materials constituting the works decisively. Finally, there are the other traditional physical factors such as the rain with its washing action; the insolation that causes thermal gradients; the saline solutions, which from the ground go back to capillary pores in the walls; and the wind that produces a scraping effect.

At last, there are causes of biological nature, both microbiological (lichens, fungi, algae, bacteria) and macro-biological (vegetation).

All these causes, described above, operate individually or combined and evolve both in conjunction with seasonal changes both according to the anthropic activities. For this reason, for understanding and quantifying the impact of the environmental parameters, natural and artificial, on the materials is necessary to measure the punctual values and their seasonal fluctuations.

Many authors [55]–[57], to simplify the study of environment-material interaction, categorize the alterations in the function of the kind of damage, which could be labeled as optical, physical mechanic-chemical and morphological alterations.

- Optical alterations influence visual parameters, such as color, luminosity, etc. [58].
- Physical-chemical and Physical-mechanical alterations. The first causes a hydrophobic and hydrophilic characteristic and porosity [59] variation,

while the second determines a decrease of adhesion, elasticity and cohesion [60];

- Morphological alterations can involve dimensional variation (i.e., torsion, expansion, etc.), material losses and discontinuity (crack and holes) [61];

According to this classification, in the subsection below we discuss the most significant parameter.

Temperature and Moister level

As shown in many articles Relative Humidity (RH) and Temperature (T) are leading causes of degradation of cultural heritage [62], [63] if they are not adequately controlled. Both play a fundamental role in all of the previously mentioned mechanisms (mechanical, chemical, mineralogical and biological).

In particular, changes of Temperature induce a: thermal expansion (significant for the structural stability of monuments and buildings); granular disaggregation of stones with amorphous crystalline texture (marbles or granites); acceleration of chemical reaction.

Relative Humidity is the main responsible for metal corrosion; fading of dyes; decreasing material resistance and in general of deformation of objects (expansion and compression). The combination of both parameters is the key factor in determining the habitat biological life.

Gaseous pollutants

Some air pollutants exist in the gaseous phase at ambient temperature [64]. Most significant gaseous pollutants that contribute to the alteration are SO_x, NO_x, CO_x and O_3 [36].

- SO_x [65] and NOx [66], [67], in the presence of humidity can turn into Sulfuric acid; Nitric acid and Nitrous acid. These acids are dangerous for metals, materials based on carbon calcium, cellulose and silk.
- CO_x [68] in the presence of humidity can turn into Carbonic acid. This acid is hazardous for objects based on carbon calcium as it starts the carbonization process [69].
- O_3 [68], [70], [71] oxidation of organic materials.

Exist a minor set of pollutant with a corrosive effect [72] of silver [73] (H_2S), copper (NH_3) [74] and bronze (HCl) [75], which are products of the secondary reaction.

Particulate Matter

As shown in [28], [36], [76]–[79] particulate matter represents an important factor of artworks deterioration and intelligibility of materials. Currently, the particulate matter is in prevalence characterized by coal, semi-soluble saline solutions (nitrates and chalk), half-combusted oils and hydrocarbons with high molecular weight [80]. They can react with other pollutants [81] or with the artwork's surface. The deposition can produce a dirtying and darkening of the surface and at last corrosion [82], [83] of the exposed material, an increasing of biological attacks (mold, bacteria and other microorganisms) [84], [85]. The particles compound is defined according to sizes [80]: total suspended particles (TSP), particles with a mean aerodynamic diameter of 10 μm (PM_{10}), particles with a mean aerodynamic diameter of 2.5 μm ($PM_{2,5}$) and fine particulate with a diameter less than 2.5 μm.

Light intensity

Light radiation natural or artificial [86], in all its component of infrared (IR), the visible band (VIS) and ultraviolet (UV) can increase different deterioration

mechanisms [87] like: color fading or blackening [88], [89]; development of biological life [90], [91]; oxidation (it has a catalytic function) [92].

Air Flow

Wind is the primary reason for loading and mechanical damage of structure [93]. Nonetheless, it can also decrease and increase the biochemical reaction of gases and/or water on the historical object. The air movements around historic structures considerably impact biological colonization, the deposition of pollutant, or the wetting-drying cycle [94]. Substantially winds transport salt, gases, dust and moister and could have an abrasive effect [95].

Vibration

Vibrations can carry out a hazard to cultural heritage objects for an assortment of reasons [96]. They could be a cause of reasonably outsized strains of objects and could origin: (i) the fallen of objects, (ii) the detachment of objects from monuments, (iii) the ruins of monuments [97], [98].

The strains have many effects and may aggravate a pre-existing mechanical faintness (opened fissures both at interfaces and at joints). Pre-existing holes or craquelures increase with recurring strains produced by vibrations. It means that letdown may be subject to the number of cycles at a specified shaking level and not upon the first instance of achieving a particular level [99], [100].

In this dissertation, we focus our attention on the temperature and moister level variation, SO_x, NO_x concentration and structural vibration due to their effects on cultural heritage conservation [101].

Part 2: Laboratory Tests

After a review of state of the art regarding the different sampling device applied in cultural heritage and a survey of the parameters that involve a degradation effect on the materials, in this section, we focus our attention on a sensors-based prototype able to detect: (i) temperature and relative humidity; (ii) NO, NO_2 and SO_2; (iii) vibrations.

In particular, this section describes the design and the validation of the Wireless Sensor Network (WSN) propose [3] *, named WENDY, an acronym for Wireless Environmental moNitoring Device prototYpe.*

WENDY, built on a microcontroller of ATmega328P series, gathers signals from a sensor for temperature and relative humidity; a 9-axis MIMU; and three gas detection miniature boards (NO, NO_2 and SO_2). Complete the board a connector for memory card (SD) and an RTC. Additionally, a module based on the ZigBee standard could be used to transmit all data. In this section, precisely, we present the performances of the WSN node in detecting: structure tilt, vibrations and the daily cycle of humidity, temperature and gas deposition.

The experimental setup used to evaluate the accuracy of MIMU system highlighted a relative error on shock acceleration measurement, in term of normalized root mean square error, lower than 0.1 % for the sinusoidal input and 0.51 % for cardinal sin input, with an average accuracy in the principal peak reconstruction of 1 % in the chosen frequency range (5 Hz to 50 Hz). The MIMU accuracy for tilt measurement, evaluated through the root mean square error was equal to 0.3° and a standard deviation always lower than 0.4° in the 0-90° tilt range. The gas detection and temperature/ humidity boards showed data comparable with the nearby certified ARPA system device.

[3] The text in this section was adapted and integrated from the papers:
"D'Alvia et al. doi: 10.21014/acta_imeko.v6i3.454"
"D'Alvia et al. doi: 10.1016/j.measurement.2018.07.004"

The developed system allows for prioritization of intervention both for management and interventions planning, regarding conservation, consolidation and restoration.

INTRODUCTION

In Section 1 we have discussed as a preventive monitoring permits to control the sustainability and durability of the artwork conservation [102], in this section, we focus our attention on the realized monitoring device.

The deterioration, as we know, is dependent on the nature of cultural heritage and it is exposed to the influence of many parameters [103]–[106]. For instance: (i) gaseous pollutants (SO_x, O_3, CO_x, NO_x) and particulate matter; (ii) relative humidity and temperature; (iii) radiation; (iv) airflow velocity and direction; (v) sound pressure and vibration [46], [56], [57]. Consequently, both long-term monitoring of the environmental parameters and further analysis of the recorded data are necessary.

In fact, in the case of cultural heritage, the environmental monitoring is typically achieved by a data storage, with a recommended rates in a range between one sample per hour (1 sample/h) or daily (1 datum/day) [107] monitoring.

Under this hypothesis [108], the development of a monitoring system based on a wireless sensors network (WSN) presents different and valuable pros. For example:

- the absence of wired invasive infrastructures or cables;
- quick and straightforward architecture scalability;
- the possibility to integrate heterogeneous and multiple sensors into a single small node;
- the capability to distribute a high number of the low-price measurement point in the historic site;
- the cooperation among the nodes for coverage extension and user interaction;
- the high lifetime;

- the low cost of the hardware platform.

As shown in different papers, currently, many remote control systems for data acquisition applied to cultural heritage are developed [109], [110].

This work starts with the priority of a data-logger with a low-price able to save data of different variables from wide spaces for particular applications as the preventive conservation. A sensor-based device that uses a 2-Wire protocol to communicate with sensors is presented [111]. It is programmed to set the correct rate of data sampling meeting with the requirements of the market and standard recommendation. In particular, we have developed a novel, low-cost, wireless, scalable system, capable of controlling environmental parameters, as well as vibrations and deformation, temperature and humidity, gaseous pollutant, over a multi-stage research project, combining MEMS sensor boards and electrochemical-cells. In this dissertation section, we present WENDY and the validation setups for a) detection of tilt and shock and define the frequency limit, b) acquisition of the daily cycle of environmental pollutant.

MATERIALS AND METHODS

Hardware

The WENDY device is developed starting from both protocols of communication and the sensors technologies. It is based on a PCB ad-hoc designed, to reduce costs and dimensions of the device compared to commercial development boards (Arduino UNO, UDOO, etc.) which require external shields for each adjunctive function (ex. SD card for data logging, Real Time function, etc.). Also, we could integrate different sensors without limitation imposed by the producer (ex. Libelium). Moreover, our solution is a low-power device compared to RaspberryPI [2].

As shown in Figure 1, the device is based on a computational unit that embeds a RISC Microcontroller AVR ATmega328P (a). The solution also integrates (b) SO2-A4, NO2-A4 and NO-A4 Alphasense sensors [112]–[116]; (c) a BME280 Bosch Sensors (Pressure, Relative humidity and Temperature PRhT)

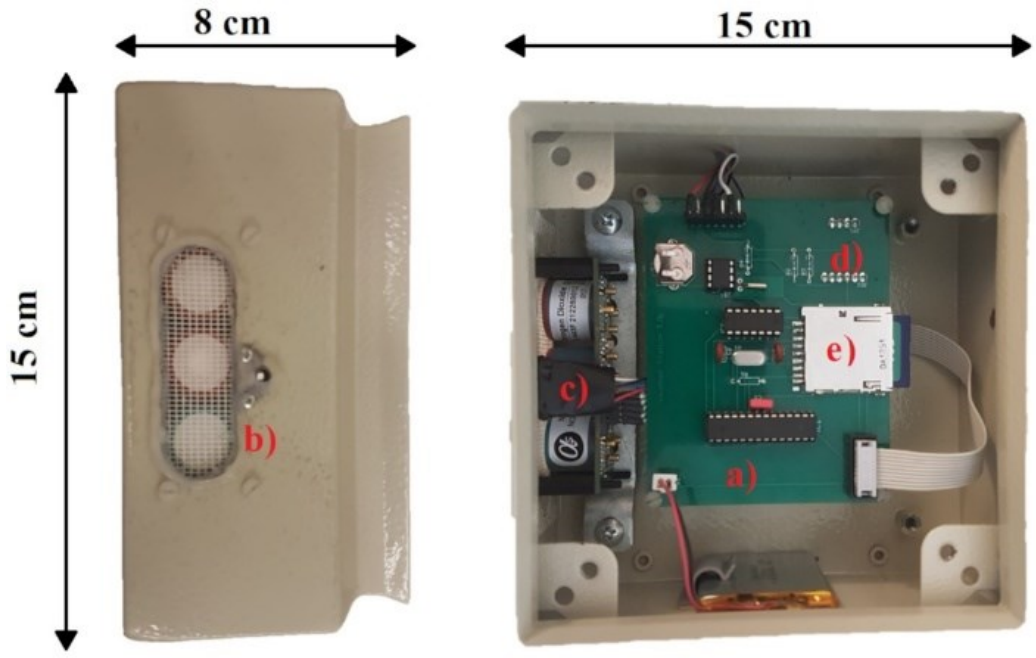

Figure 1 The system with highlighted the components: a) microcontroller board, b) gas sensors, c) BME280, d) BMO055, e) RTC and storage SD card system and the dimension.

development board [117];(d) BNO05 Bosh sensors development board [118]. A connector for memory card (SD) and an RTC ds1337 are added (e). All sensors are connected to the microcontroller via an i2c serial communication bus. The system is completed with a transmitting/receiving ZigBee unit.

Microcontroller ATmega328

The proposed wireless node is based on a Microcontroller (MCU) ATmega328P, chosen to dispose of an environment simple to program and that implements in C++ all the libraries.

It is a low power microcontroller with one I2C port used to connect all chosen sensor boards and the external clock; one SPI serial interface accustomed to connect the external SD memory and one programmable serial USART used to interface the MCU with an external PC for programming or radio-transmitter.

The microcontroller ATmega328p is chosen due to the 0.2 mA in Active Mode low power consumption at 3.7 V and the low cost. Additionally, the modality of Power-Down Mode (0.10 μA) and Power-Save Mode (0.75 μA) are provided and used. Moreover, we choose this microcontroller due to the simplicity of *bootloading* and the availability of libraries in the creative common right for the chosen sensors. Moreover, the programmable memory of 32 kB and EEPROM memory of 1 kB is enough to store all the necessary libraries, the main program and sensors output respectively.

Power Supply

A Li-ion battery with a capacity of 2 Ah, which guarantees forty days of functioning power the entire system is powered.

Radio Module

The Radio Module is a transmitting/receiving ZigBee unit IEEE 802.15.4 in 2.4 GHz band with +3dB output power and 250 kB/s transmission. It is used in AT commands directly connected to the USART of the ATmega328P.

Plug-in for Sensor Boards

The MIMU (Magnetic Inertial Measurement Unit) BNO055 is a low-cost sensor that integrates a 3-axis geomagnetic sensor, 3-axis gyro and a 3-axis accelerometer. It is possible to setting-up different factors as the g-range; the cut-off frequency of low-pass filter, or the interrupt signal generation if a particular event occurs (a changing in angular or in linear acceleration). The MIMU has a max power consumption at 3.7 V of 0.2 mA. We have chosen it due to the low-cost and the versatility of internal fusion-algorithm that permits the offset calibration of the sensor, the monitoring of the calibration status. Additionally, Kalman's filter provides the distortion-free and refined orientation of the output vectors.

The MEMS BME280 is a low-price sensor that combines digital temperature, pressure and humidity sensing elements. It measures temperature (T) in the range -40 °C to 85 °C with an accuracy of 0.5 °C, Percent Relative Humidity (%RH) in the range 0% to 100% with an accuracy of ±3% and Pressure (P) in the range 300 hPa to 1100 hPa with an accuracy of ±1 hPa. We have principally chosen it due to the low-cost and the versatility of three-in-one sensors. At 3.7 V the power consumption is 0.2 mA.

Alphasense 810-0019-03 model is a three-input analogic front-end sensor board mounting SO2-A4, NO2-A4 and NO-A4 electrochemical cell for SO_2, NO_2 and NO gas concentrations. In particular, the NO-A4 and the NO2-A4 present respectively a sensitivity of 0.404 mV/ppb and 0.267 mV/ppb in the range of 0 ppm to 20 ppm, while the SO2-A4 a sensitivity of 0.267 mV/ppb in the range of 0

ppm to 50 ppm. We have chosen it because the system is calibrated and certified by the producer that gives to the user all the information needed to compensate both zero and sensitivity drift for each sensor. The Alphasense 810-0019-03 board is connected to the main microcontroller (ATmega328p) through an analog-to-I2C converter. The power consumption of 810-0019-03 board model and the four sensors is two mA at 3.3 V. All sensors have been chosen according to the values present in the literature [90], [119]–[121], as Table 2 shows.

External Clock

The real-time clock ds1337 allows acquiring and organize the data in a different format of output: calendar (days, months and years), times (seconds, minutes and hours), or complete. Also, ds1337 allows the possibility to generate two interrupt flags associated with two different time alarms: Alarm1 and Alarm2. Alarm1 works in the seconds-days range, while the second Alarm2 works in the minutes-days range. The I2C protocol is the communication protocol used to transfer data to the microcontroller. The chip has a dedicated power supply (CRC1220 3.3 V Li-ion battery) to guarantee a no time reset when the device is not powered.

Table 2 Parameters, Measurement Units, Range of Tolerance

Parameter and range for Risk Analysis		
Parameters	Unit	Range of tolerance
ΔT	°C	depends on the material
ΔRH	%	depends on the material
SO_2	μg/m^3	500 at 10 minutes avarage
NOx	μg/m^3	200 at 8 hours average
p.p.v.	mm/s	Depends by frequency

External Memory

All acquired data are saved into a data-logger based on an external Secure Digital memory card (SD). The SPI port is used for the communication between SD ad microcontroller.

Design of Hardware and Software

We realized the printed circuit board (PCB) using the free software "Eagle CAD". The width of the tracks and the minimum distance between them have been chosen equal to 1.27 mm, in a conservative way, in a double layer. The PCB was etched on an FR4 board with a thickness of 1.6 mm and 100 mm × 80 mm. Both layers are characterized by a ground plane. Figure 2 shows the schematic of WENDY device.

The C++ Computer language has been adopted for the writing of all algorithm programs. All the programs are designed using Arduino IDE and commands. The detailed firmware used for the "Monitoring of Minerva Medica" will be discussed in Appendix A - Code.

The final firmware, moreover, holds an interrupt routine to including a data buffer to overcome the communication timing jitter during the data communication on the i2c serial (50 Hz) for the BNO055 sampling frequency.

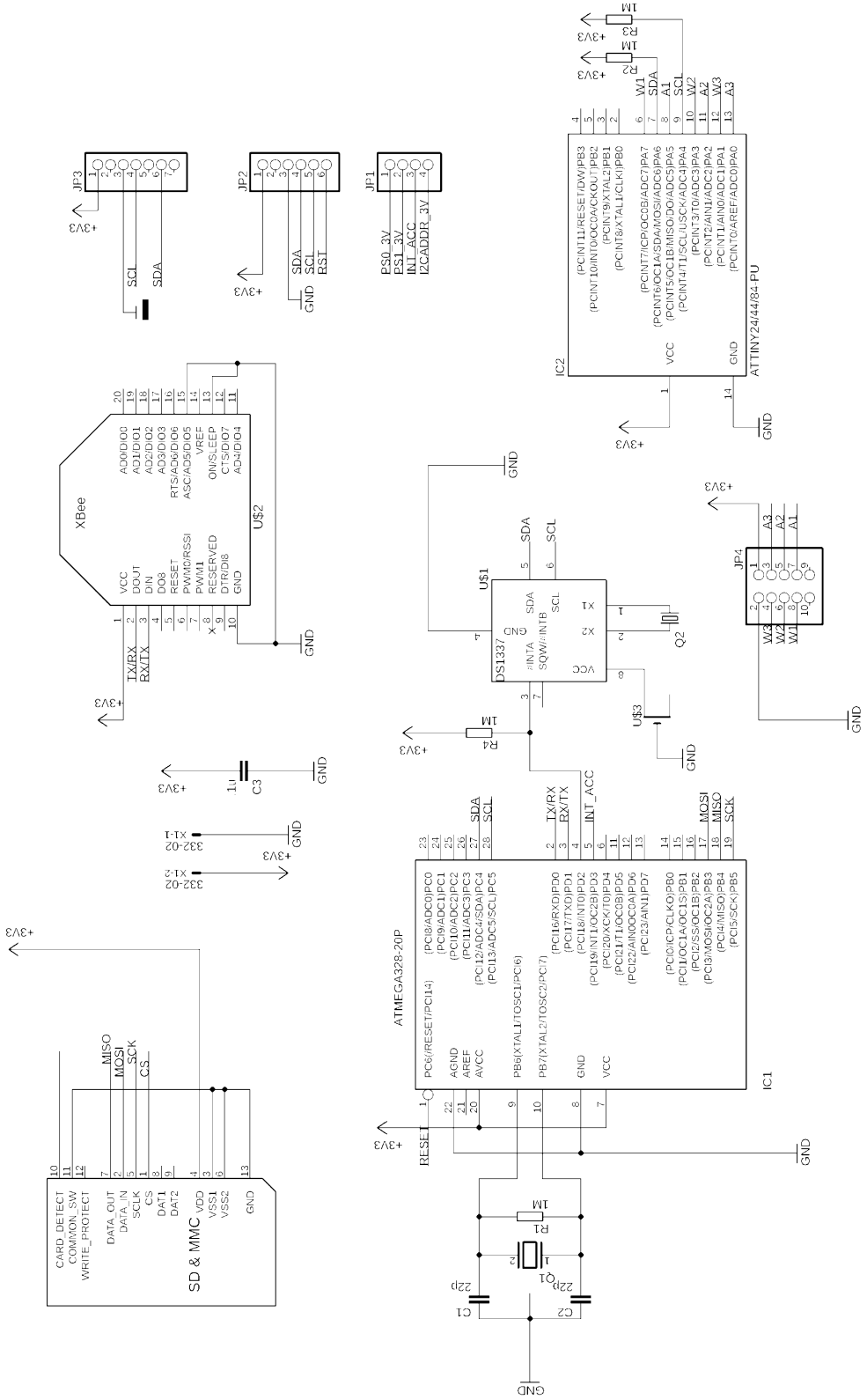

Figure 2 WENDY schematic.

Experimental procedure

The MIMU sensor is employed for two monitoring activities: (a) shock detection and (b) tilt detection of the wall due to fracture and/or deformation. To assess the performance of the MIMU in these two applications, two different experimental setups have been designed: (i) the former including an electro-dynamic shaker and (ii) the latter including a rotating plate. In our node prototype, tilt and shock will be detected by different processing data from the same inertial sensor. For this reason, we set a cut-off frequency for the in-built settable low-pass filter at 250 Hz, a high value for tilt, but required for properly acquiring vibrations. The environmental sensors, for hydrothermal values and pollutant concentration, have been placed outdoor, for evaluating the system in proximity of a certified pollution monitoring system by ARPA Lazio (Lat. 41.864194°, Lon. 12.469531°).

Shock detection

The UNI 9916 recommendations describe variables and methods to measure vibrations and their effects on a building, either modern or ancient, identifying two key parameters: the peak particles velocity (p.p.v) and the peak component particles velocity (p.c.p.v). The p.p.v-value represents the maximum value of the magnitude of the velocity vector measured at a given point while p.c.p.v-value is defined as the module of one of the three orthogonal components measured simultaneously at one point. Moreover, both values could be directly measured or obtained by integration of acceleration data.

The relation between magnitude and frequency of the vibration signal is summarized in Table 1. Especially the chosen range relates in this study the range 0 Hz to 50 Hz is investigated allowing the results of other works in the filed [122], [123].

Before the application of the instrumentation on site, we conducted a validation session in our lab. In particular, we focused our attention on the accuracy of MIMU, applying both sine and cardinal sin (sinc) waveform to a Vibration Exciter Type 4809 (Bruel&Kjaer), used to provide a controlled input to the sensor. We compared the output of the filtered (250 Hz cut-off) MIMU output with a reference signal provided by a certified mono-axial accelerometer (Bruel&Kejar 4371 model.) Both sensors have been placed on top of the Vibration Exciter as shown in Figure 3.

A high accuracy waveform generator has imposed the *sine* and *sinc* motion and the amplitude of the gain was set to produce the maximum velocity acceptable for the chosen frequency. The test for the sin signal has been repeated for five different frequencies (5 Hz, 15 Hz, 25 Hz, 35 Hz and 45 Hz), range compatible with other studies in the field.

For the *sinc* signal, chosen as it best reproduces the vibration caused by the public transportation nearby the monument, we chose to test the signal at 5 Hz, 15 Hz and 25 Hz according to other studies in the field [123]–[125]

The described procedure has been repeated three times by aligning each time a different MIMU axis with the motion axis.

Table 3 p.c.p.v an p.p.v maximum values, according to the UNI 9916, in relation with the frequency of vibration at ground level for historic building

Ground Level			
Frequency (Hz)	< 30	30 – 60	> 60
p.p.v (mm/s)	6	8	12
Frequency (Hz)	< 10	10 – 50	> 50
p.c.p.v (mm/s)	3	3 to 8[a]	8 to 10[b]

[a.] Linear relation

[b.] Linear relation; over 0.1 kHz a speed of 10 mm/s is used as reference value.

The TYPE 2692-c (Bruel&Kjear) can integrate the accelerometer signal and evaluate the velocity. Thus, we set the proper velocity amplitude for the chosen frequency. In the post-processing phase, we compared the acquired signal of 4371 model with the signal acquired and integrated through MATLAB, of BNO055.

Accuracy has been evaluated by calculating the RMSE between test and reference signals, normalized to the peak-to-peak value of the reference sensor (nRMSE), as reported by Equation 1.

$$\mathrm{nRMSE}^{x,y,z} = \frac{\sqrt{\frac{\sum_{i=0}^{n}\left(s_{ref}^{x,y,z} - s_{test}^{x,y,z}\right)}{n}}}{\max\left(s_{test}^{x,y,z}\right) - \min\left(s_{test}^{x,y,z}\right)} \quad (1)$$

Also, we had determined the accuracy in the central peak reconstruction, when the sinc input was applied. In particular, we have evaluated the residual between the corresponding peaks in the two signals and then calculated the

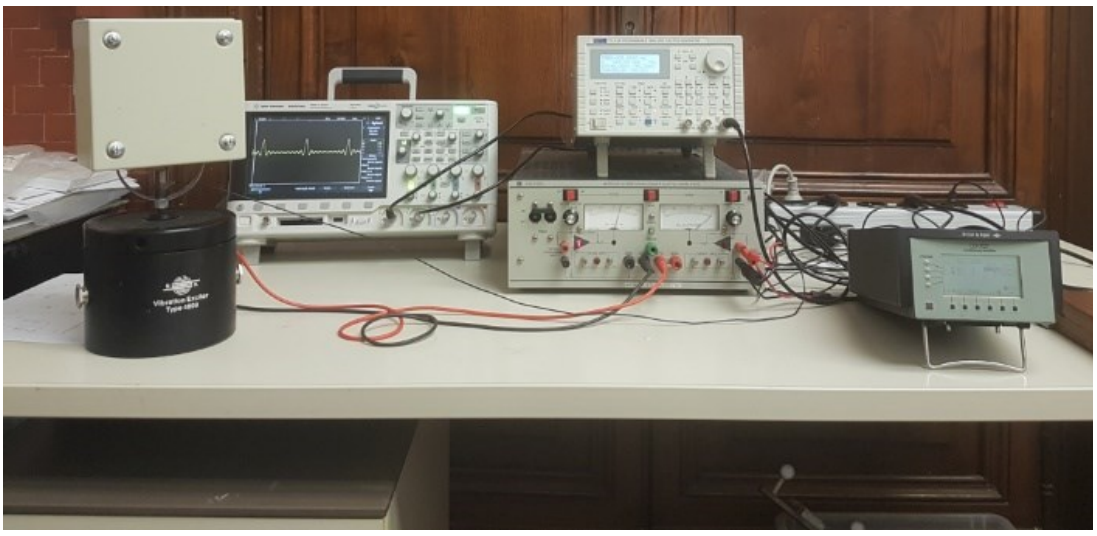

Figure 3 The experimental setup, with Vibration Exciter Kjaer Type 4809, mono-axial accelerometer Bruel&Kejar 4371 model, charge amplifier Bruel&Kjear TYPE 2692-c (Bruel&Kjear), signal generator and WENDY device.

average of the absolute value of the residuals as a percentage of the reference value for each frequency.

Tilt detection

A servomotor controlled in a closed loop using an angular encoder (Sanmotion rs1a03aa) has been used to estimate the accuracy and the stability of the embedded accelerometers. Correctly, the MIMU was mounted on a vertical plate connected to the servomotor through a belt as shown in Figure 4.

The BNO055 has been programmed by setting the internal low-pass second order filter to 250 Hz and the measurement range to ±16 g (same parameters were selected for vibration detection test).

A LabVIEW program has been implemented to rotate the plate around the horizontal axis from 0° to 180° with a step of 1° every 15 minutes, simulating tilt

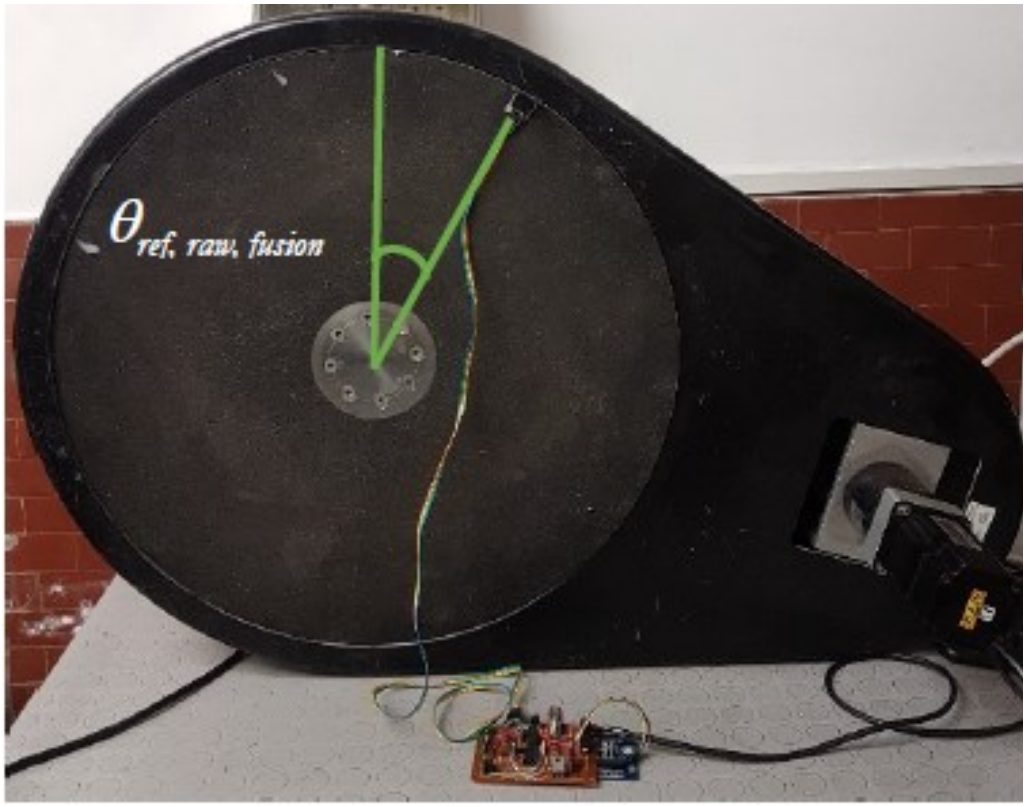

Figure 4 Plate with highlighted the θraw, θfusion, θref angles.

rotations induced by structural deformations. We acquired tilt angles measured by the encoder (θ_{ref}), the roll angle (θ_{raw}) calculated directly by three acceleration components ($\boldsymbol{a_x}$, $\boldsymbol{a_y}$, $\boldsymbol{a_z}$) and the roll angle provided by the data fusion algorithm that is embedded into the sensor (θ_{fusion}).

To validate the goodness of the built-in sensor fusion algorithm, the accuracy of the accelerometers was estimated using the Root Mean Square Error (RMSE) between the average values of the measured signals (θ_{raw}, θ_{fusion}) in the 15 minutes' window and each reference angle (θ_{ref}), gathered every 15 minutes. The standard deviation of θ_{raw} was evaluated to estimate the noise of the accelerometers, an important parameter to avoid misdetection, due to long-term functioning of the sensor.

Environmental parameter

In the preliminary test, we decided to put the sensor system outdoor, in the proximity to a certified monitoring system (ARPA), during a five-days acquisition. The system has been programmed with a sample period of 10 minutes, to evaluate the accuracy of the sensor output in mutable meteorological and traffic conditions. The acquired data have been post-processed by calculating the moving averages of the outputs with a one-hour step and an 8-hour window (8h-Average).

Regarding gas concentrations, the temperature dependence is corrected in post-processing using the output of the embedded Pt100. Corrected gas concentration values are calculated using the formula provided by the calibration certificate.

RESULTS AND DISCUSSIONS

Results of Shock and Tilt Detection

Shock Detection

Figure 5 and Figure 6 show the comparison between the reference acceleration $\boldsymbol{v}_{ref}$ and the test acceleration $\boldsymbol{v}_{test}$, in correspondence of all excitation frequences, rispectively for sin and sinc signals. From the analysis of figures, it clearly appears that the phase shift between the acceleration measured through the MIMU and the one measured with the certified accelerometer is negligible, despite the difference in signal filtering. MIMU uses an internal second order low pass filter, with undeclared parameters, while we applied a second order Butterworth digital filter, with a 250 Hz cut-off frequency of the certified accelerometer signal. In addition, to obtain the output in term of velocity, the accelerometric signals are integrated, an operation that introduces an additional phase-shift.

Figure 7 shows the nRMSE for the three axes for both signals at the chosen frequency. The nRMSE value of sin signal is similar for the three axes and it is lower than 0.1% for sin waveform. At 45 Hz we have an increase of nRMSE due to a timer jitter (without the buffer the nRMSE is always over the 36%)

The nRMSE value for the sinc signal is similar for the three axes at the same frequency, but increase exponentially with the frequency increases, the maximum value of 0.52 is, however, lower than the nRMSE evaluated without the buffer (0.59%).

Accuracy in main peak reconstruction when the sinc input was applied are 0.45%, 0.83% and 1.15% respectively for 5 Hz to 25 Hz signals.

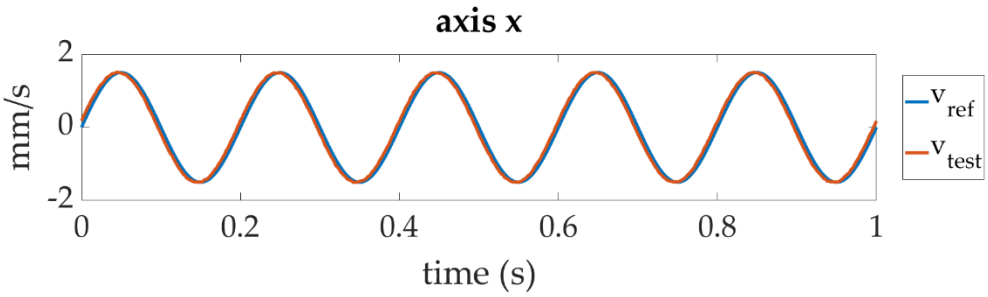

Comparison between v_{test} and v_{ref} at 5 Hz along the x-axis

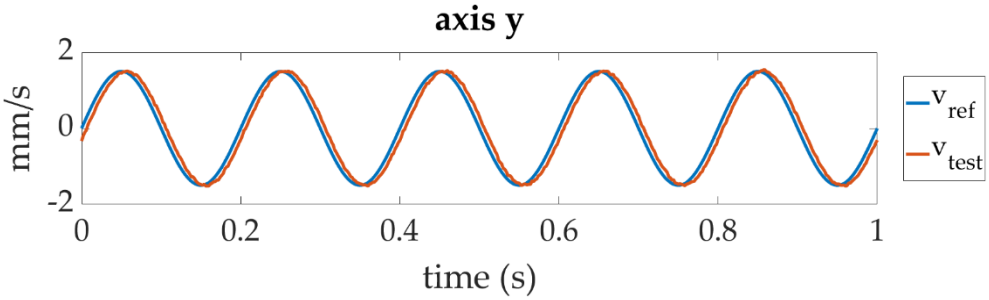

Comparison between v_{test} and v_{ref} at 5 Hz along the y-axis

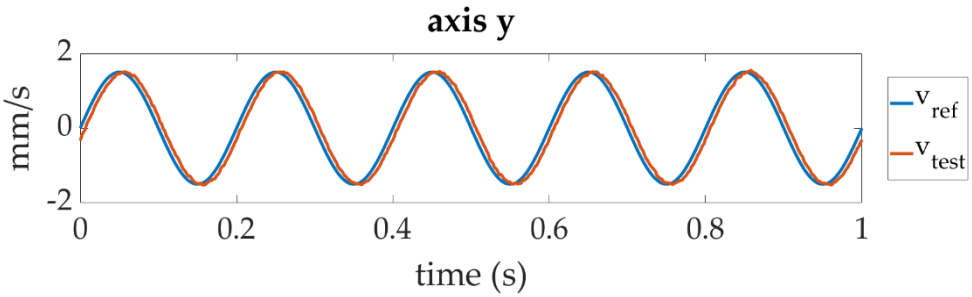

Comparison between v_{test} and v_{ref} at 5 Hz along the z-axis

Figure 5

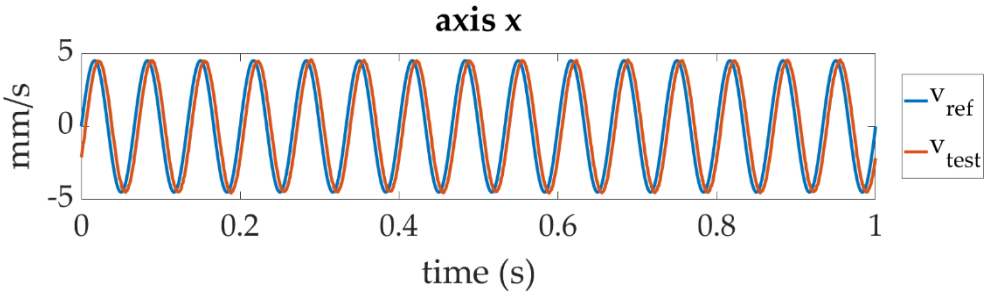

Comparison between v_{test} and v_{ref} at 15 Hz along the x-axis

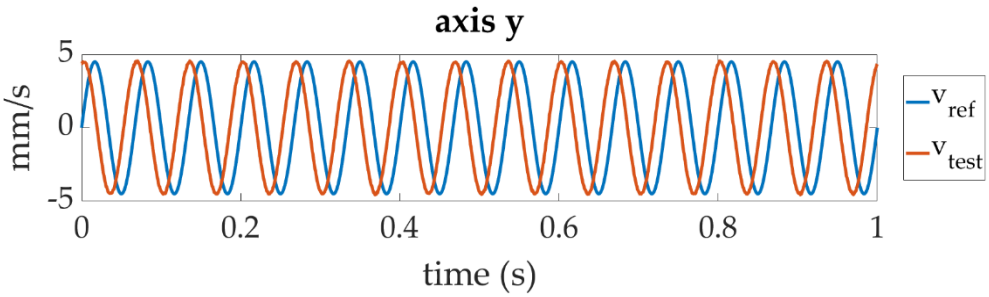

Comparison between v_{test} and v_{ref} at 15 Hz along the y-axis

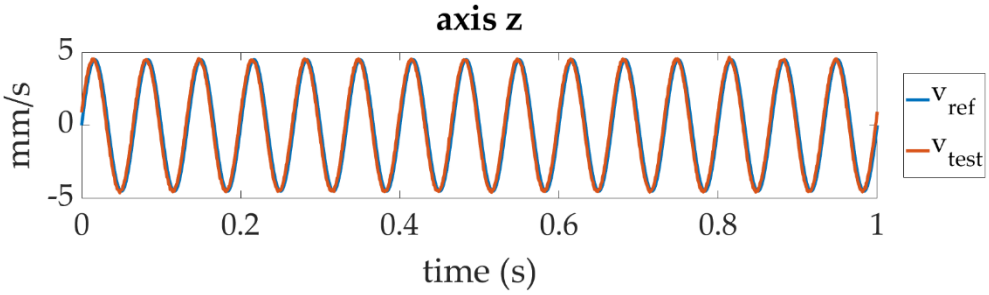

Comparison between v_{test} and v_{ref} at 15 Hz along the z-axis

Figure 5

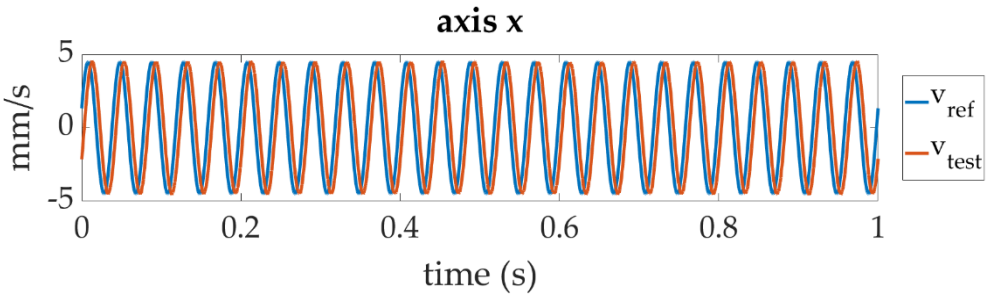

Comparison between v_{test} and v_{ref} at 25 Hz along the x-axis

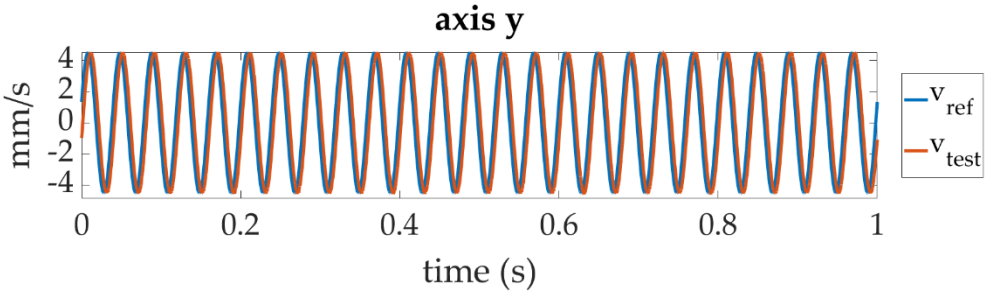

Comparison between v_{test} and v_{ref} at 25 Hz along the y-axis

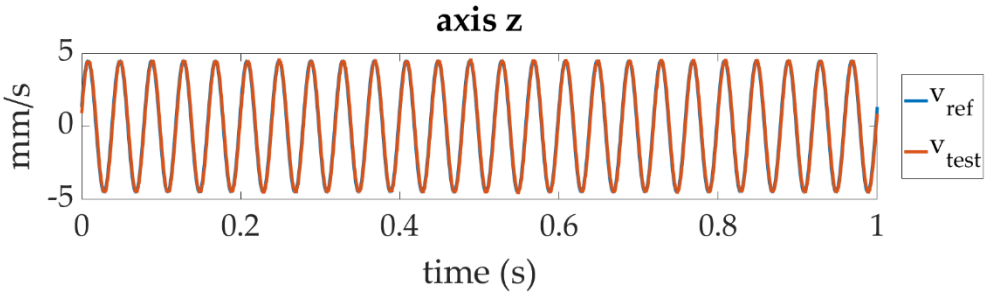

Comparison between v_{test} and v_{ref} at 25 Hz along the z-axis

Figure 5

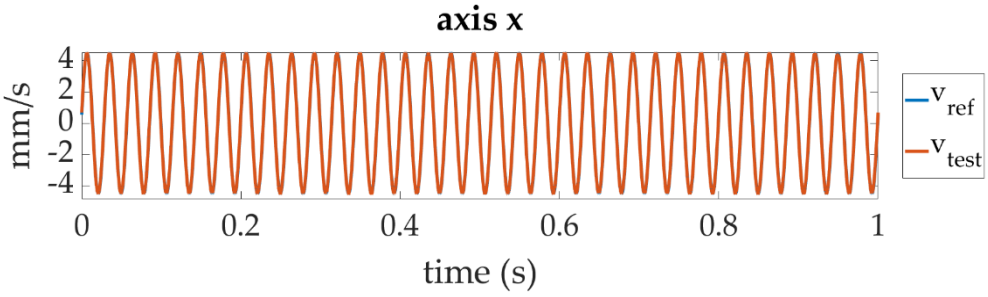

Comparison between v_{test} and v_{ref} at 35 Hz along the x-axis

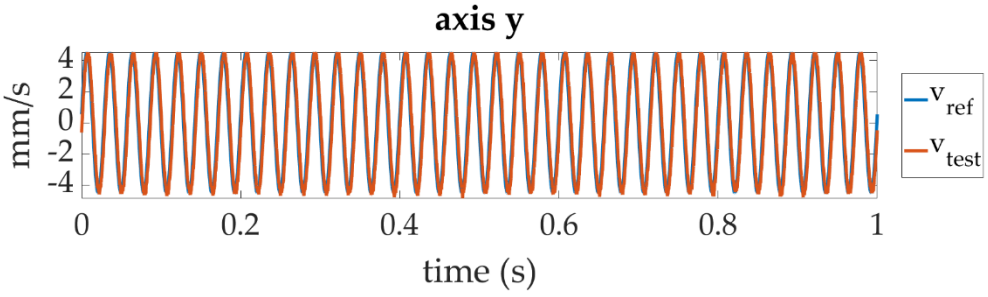

Comparison between v_{test} and v_{ref} at 35 Hz along the y-axis

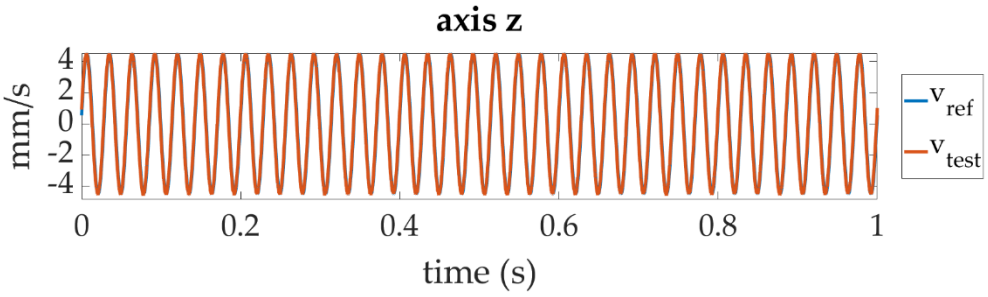

Comparison between v_{test} and v_{ref} at 35 Hz along the z-axis

Figure 5

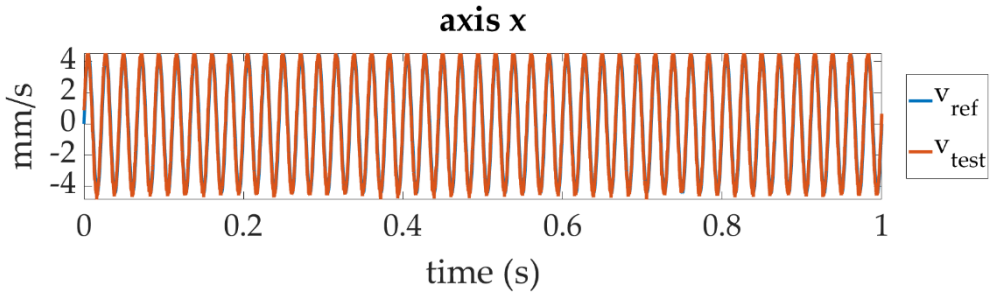

Comparison between v_{test} and v_{ref} at 45 Hz along the x-axis

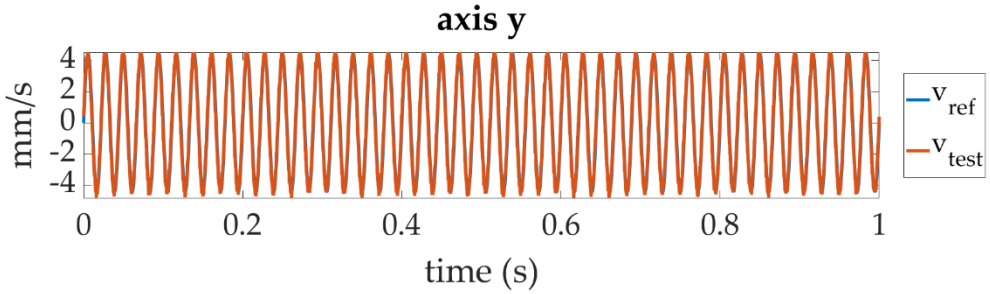

Comparison between v_{test} and v_{ref} at 45 Hz along the y-axis

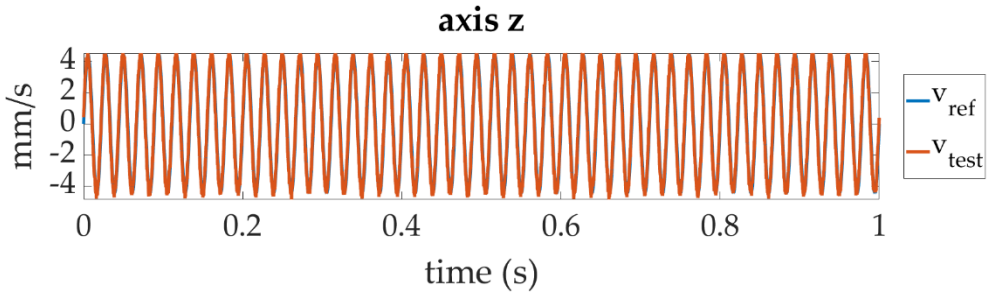

Comparison between v_{test} and v_{ref} at 45 Hz along the z-axis

Figure 5 Comparison between v_{test} and v_{ref} at 5 Hz to 45 Hz

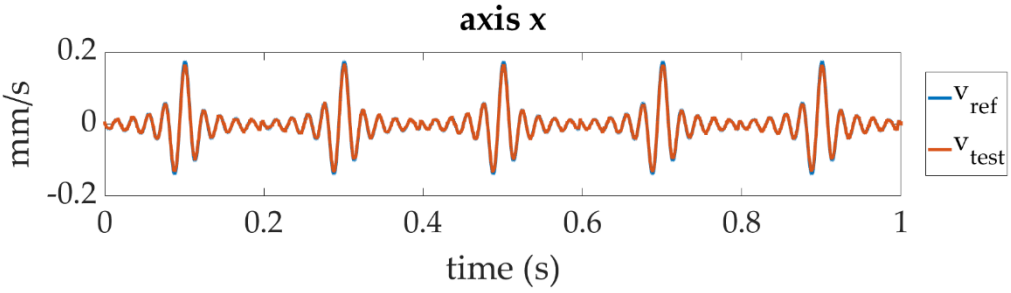

Comparison between v_{test} and v_{ref} at 5 Hz along the x-axis

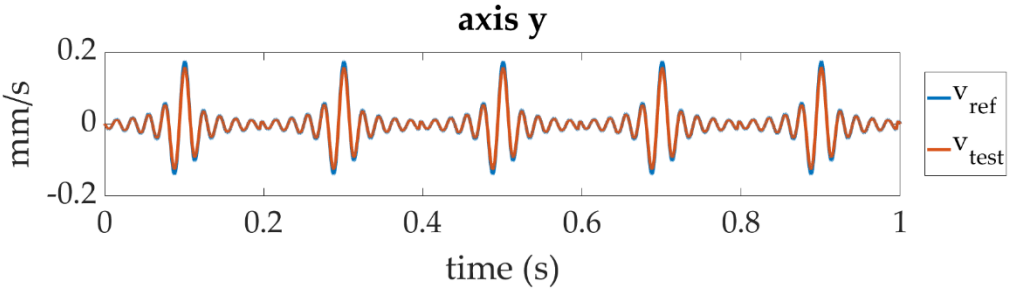

Comparison between v_{test} and v_{ref} at 5 Hz along the y-axis

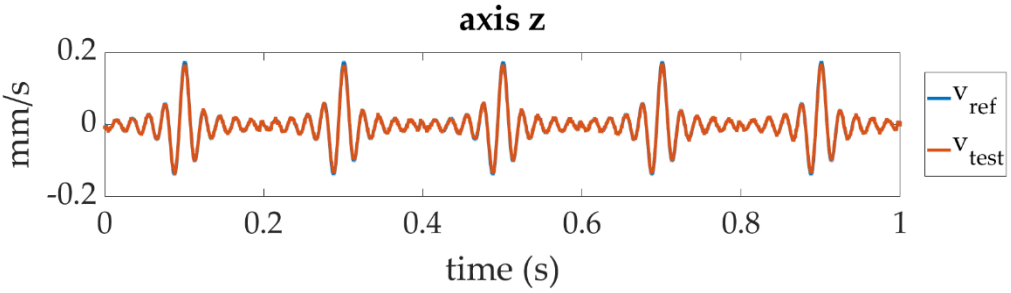

Comparison between v_{test} and v_{ref} at 5 Hz along the z-axis

Figure 6

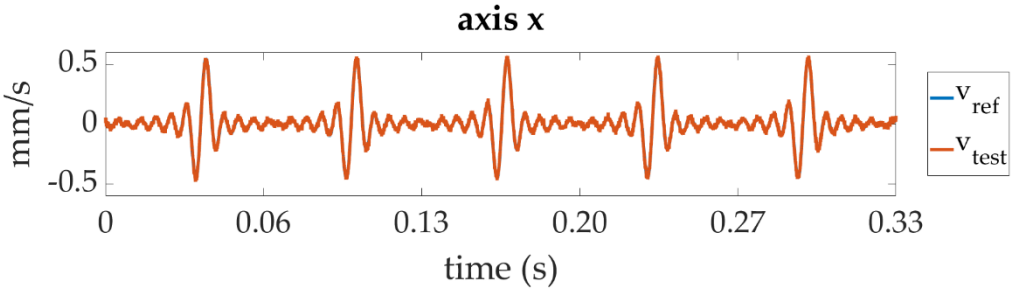

Comparison between v_{test} and v_{ref} at 15 Hz along the x-axis

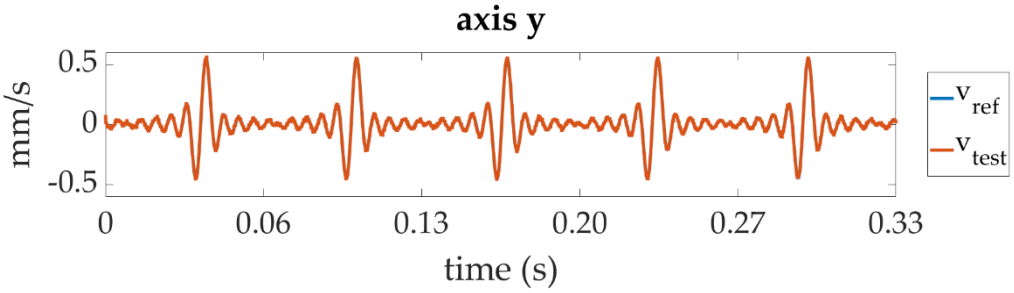

Comparison between v_{test} and v_{ref} at 15 Hz along the y-axis

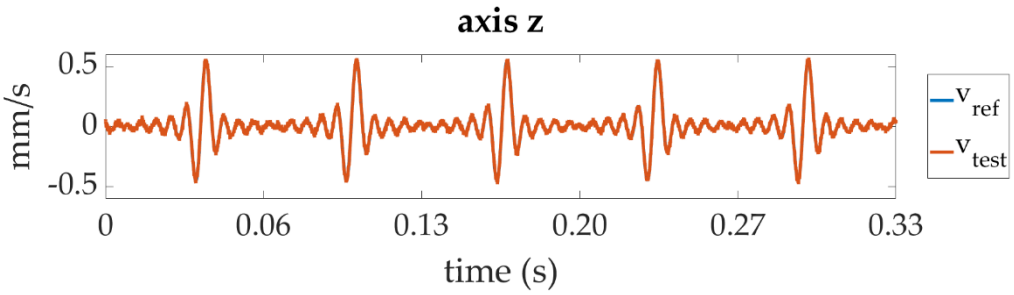

Comparison between v_{test} and v_{ref} at 15 Hz along the z-axis

Figure 6

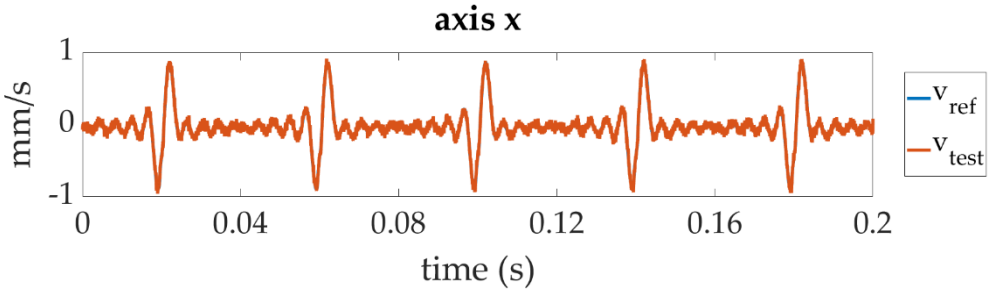

Comparison between v_{test} and v_{ref} at 25 Hz along the x-axis

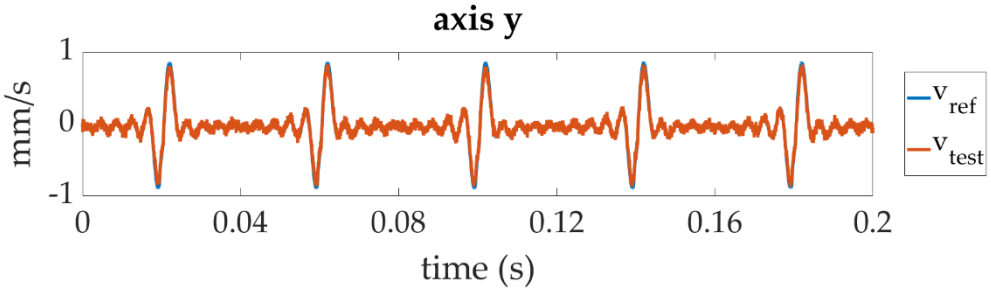

Comparison between v_{test} and v_{ref} at 25 Hz along the y-axis

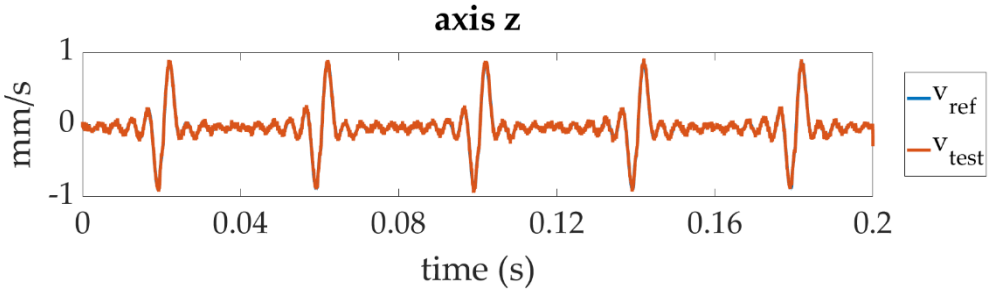

Comparison between v_{test} and v_{ref} at 25 Hz along the z-axis

Figure 6 Comparison between v_{test} and v_{ref} at 5 Hz to 25 Hz

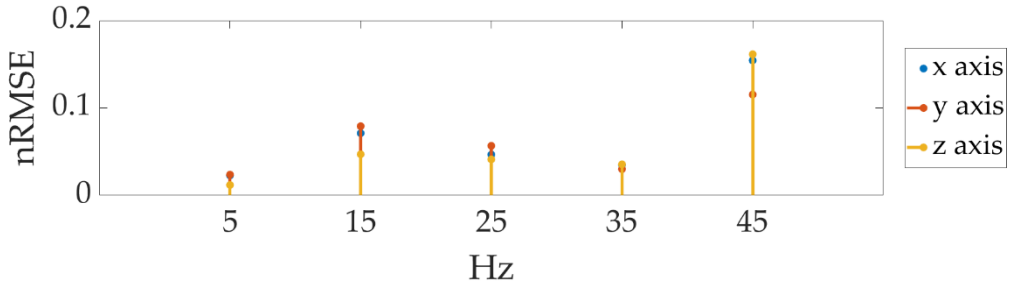

nRMSE for Sin signal.

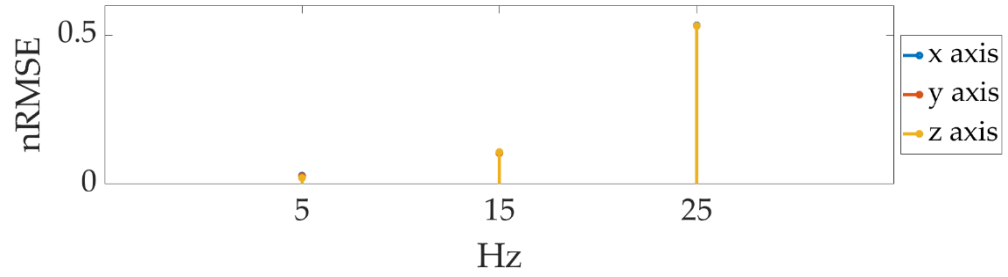

nRMSE for Sinc signal.

Figure 7 nRMSE for Sin and Sinc Signal with highlighted the respective chosen frequency

Tilt Detection

The relation between θ_{ref} and θ_{raw} is shown in Figure 9. The MIMU accuracy for this measurement, evaluated through the RMSE, was equal to 0.3°. The SD of the MIMU output was always lower than 0.4° in the 0-90° tilt range.

Figure 9 reports the test results in the 0-90° range: the RMSE between θ_{fusion}. Moreover, θ_{ref} was equal to 0.2° and the Standard Deviation StD was always lower than 0.2° in the 0°-180° tilt range.

This wide range was chosen to assess accuracy in the tilt angle measurement regardless of the initial placement of the sensor since MEMS accelerometers embedded into MIMUs can present different accuracy levels for each axis.

Figure 8 shows the comparison between θ_{raw} and the one provided by the internal sensor fusion algorithm θ_{fusion}. Figure 8 highlights how the fusion algorithm output is less sensible to noise and, consequently, more stable over time, with a maximum SD of 0.2°. The embedded data fusion algorithm, based on Kalman's filter, can filter noise; however, due to the slow dynamics of the phenomenon, the increased stability is not paid in term of noise, as demonstrated by the RMSE.

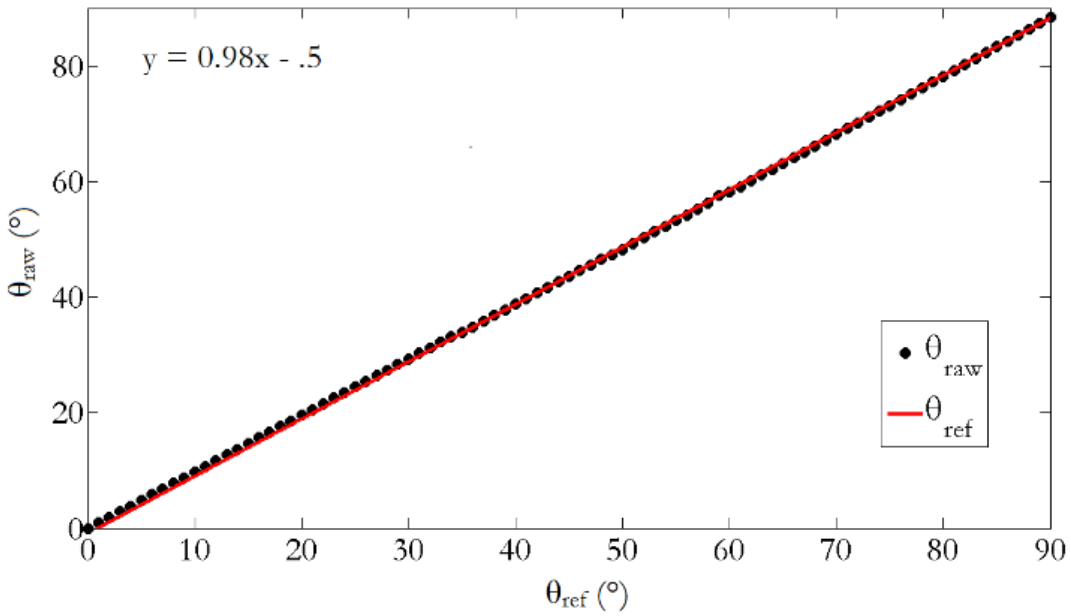

Figure 8. Example of acceleration signals acquired via the two systems

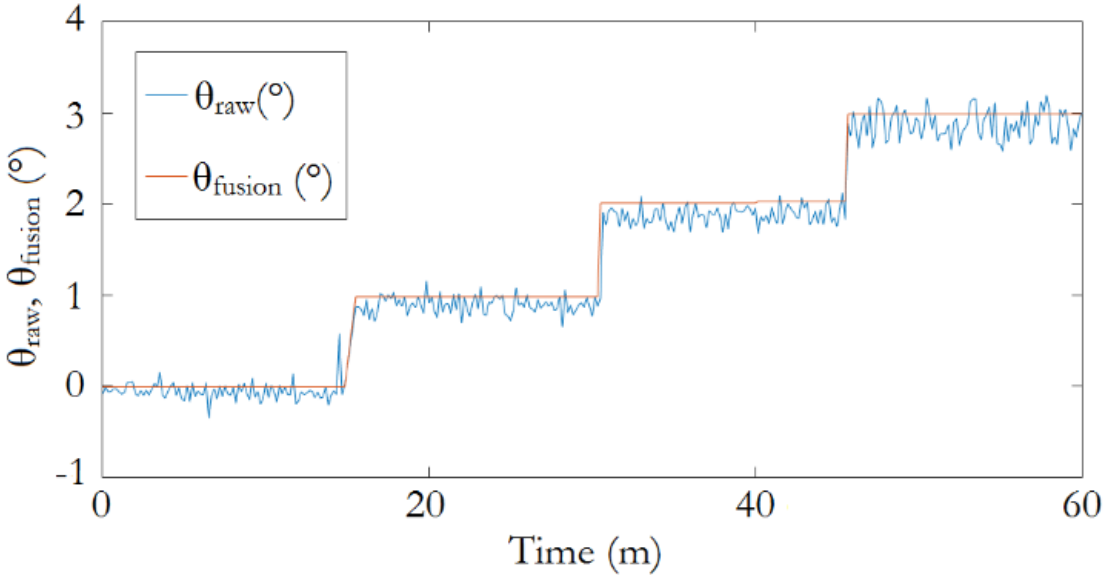

Figure 9 Evaluation of the stability between θ_{raw} and θ_{fusion} in 0-3°.

Environmental and pollution detection

Figure 10 reports the outdoor concentration of pollutant gasses in ppb in two chosen days, between 12:00 AM on Friday 02/10/17 to 12:00 AM of Sunday 02/12/17. Generally, the gaseous pollutant concentration is higher during the daytime than during the night. Values are well-matched with the concentration values given by the ARPA monitoring station [126], [127] and inferior to the normalized day limits (140 ppb for SO_2, 100 ppb for NO_2 and NO). The Arpa System reported a maximum of NO_2 hourly concentration at 7 pm for both 10 and 11 February 2017. These peaks have a time-correspondence with the ones in Figure 8, even if the actual value measured with our WSN (37 ppb against 60 ppb from ARPA system) is affected by the height difference.

The maximum level of SO_2 concentration appears to be 1 ppm. SO_2 is an impurity compound of fossil fuel commonly used in buildings.

The highest values of hourly SD were 0.7 ppb for NO_2, 0.2 ppb for NO, 0.8 ppb for SO_2.

Figure 11 shows the day-night cycle of temperature and moister level in the two chosen days, between 12:00 AM on Friday 02/10/17 to 12:00 AM of Sunday 02/12/17. As expected, the sensor shows an evident decrease in RH, in correspondence to an increase in temperature (ex. 12 AM). Maximum values of hourly SD were 0.4 °C and 0.6% for temperature and relative humidity, respectively. A certified thermohydrometer is placed near WENDY to evaluate the accuracy of the sensors. The RMSE is 0.11 °C and 0.18% respectively for temperature and percent relative humidity.

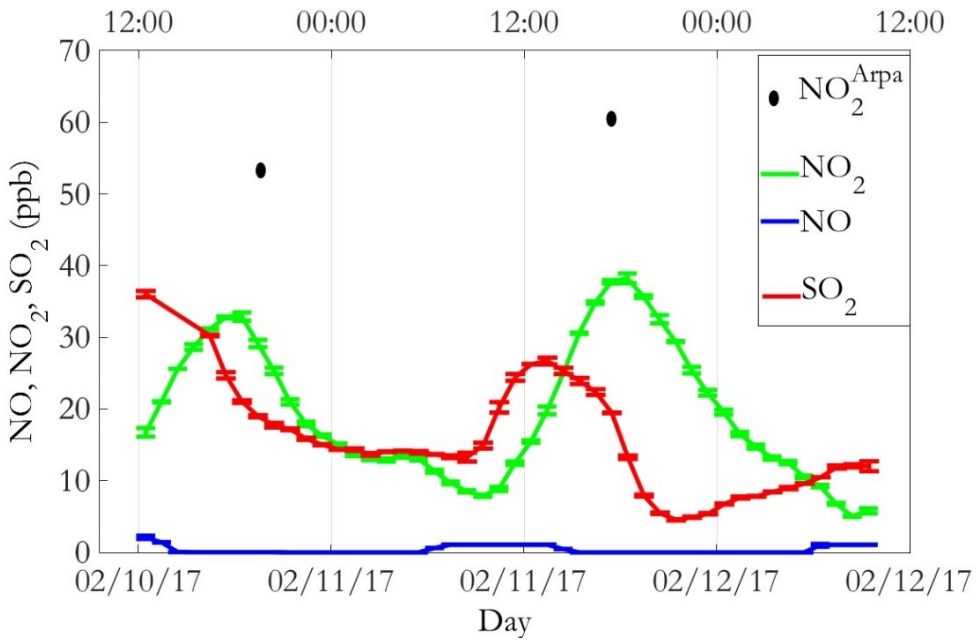

Figure 10 8h-average gas concentration for SO2, NO2, NO with 8h-SD.

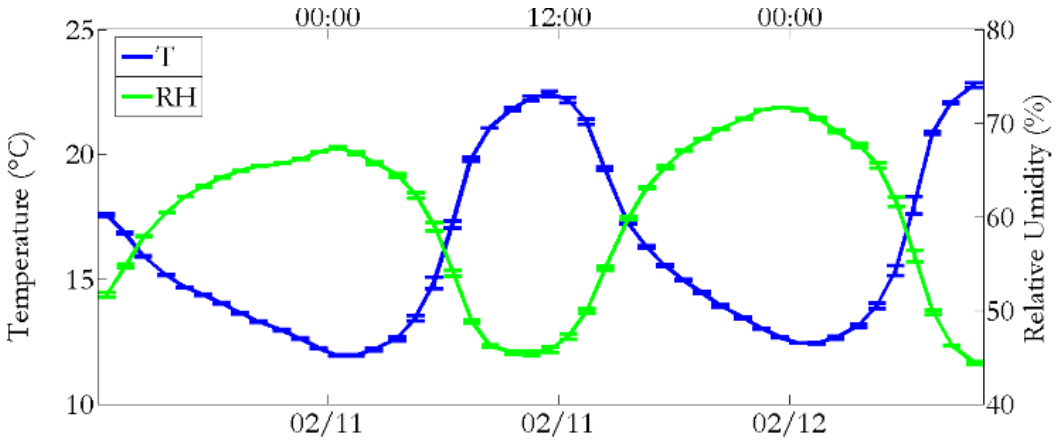

Figure 11 8h-average for temperature and relative humidity with hourly SD and RMSE.

Conclusions

We designed and analyzed the performances of a low-cost wireless sensor network node for the environmental monitoring of cultural heritage. At this stage of development, we focused on the assessment of the accuracy and stability of tilt angle and shock detection, measurement of gas concentration and thermo-hygrometric parameters.

The tilt measurement demonstrated a good accuracy for the targeted application. The observed stability was acceptable in the chosen measuring field, demonstrating the robustness of the solution as a function of time. The embedded data fusion algorithm demonstrated a good capability of filtering noise without losing responsiveness for this application.

The experimental setup for vibration detection demonstrated a stable behavior over the chosen frequency range (5 Hz to 45 Hz), along with the three different axes. Despite relative error on shock acceleration measurement is not negligible (nRMSE up to 10% in sin setup and up to 52% for sinc setup), it can be considered acceptable for shock detection due to the good accuracy in the primary peak reconstruction (lower than 1.15%).

Outdoor behavior confirmed the expected inverse proportionality between temperature and RH.

Gas concentration sensors showed a trend over time comparable to data from the ARPA system, with a time correspondence in peak values, even if a difference in average values was observable due to a different height positioning.

Despite the full operating range (0 to 20 ppm) of the gas sensors, in general, gas concentrations at street level are in the range of 20-200 ppb for SO_x and NO_x, according to the OMS guideline. Values found in this study are in line with expectations.

Alphasense's electrochemical cells present limitation due to cross sensitivity to other chemical compounds, lifetime (2 years) and drift. However, the limited cost (ca. 50 € each) allows for a massive diffusion of sensor's nodes in a limited area.

Part 3: Application on site

In this section, we proposed a measuring unit and presented the collected data. The aim of this work is monitoring effects of different factors which affect the "Minerva Medica Temple," an archeological site in Rome. In particular, we focus on: (i) the seasonal thermal variations on the structure; (ii) the contamination due to by local traffic regarding gaseous pollutant and (iii) the dynamic response of the structure to a tramway line located in Rome and called "Roma- Giardinetti." The developed system allows for prioritization of intervention both for management and interventions planning, regarding restoration, consolidation and conservation.

Moreover, the software structure of the environmental monitoring device is presented and expounded in detail.[4]

Always in this section, an innovative procedure for the evaluation of the environmental hazard in cultural heritage is proposed. This risk assessment can be considered as a "relative risk assessment methodology." In particular, it considers the impacts of microclimatic conditions on the monument, based on the international norms and the current scientific knowledge. For measurement campaigns with WENDY, the risk method proposed is applied to the results of two measurement campaigns carried out between 2017 and 2018 over two different periods (September-December and March-July), at "Minerva Medica Temple," in Rome.

[4] The text in this section was adapted and integrated from the papers:
D'Alvia et al. doi: 10.1016/j.measurement.2018.07.004
D'Alvia et al., IEEE Catalog Number: CFP18O73-USB

INTRODUCTION

In the last years, the attention to novel technologies and methodologies for the real-time monitoring for the maintenance of archeological sites and conservation of cultural heritage and artworks has increased significantly [46]. Despite the necessity for preventive conservation and remote (or local) monitoring has been widely documented, is still challenging to find a standard approach, due to the intrinsic heterogeneity of problems related to each monument or artifact [103], [109]. As widely discussed in Sections 1 and 2, outdoor environmental monitoring is based on sparse stations, holding dedicated units for capturing, processing and displaying data about macro and micro-pollutants. In general, these stations are instrumented with expensive air quality sensor devices, which provide accurate data but only in a few pre-defined locations, usually far from structures of interest, due to their dimensions [11]. The expensiveness of commercial solutions, regarding purchasing, running and maintaining costs, actually limits the number of installations. Also, the correlation of all stations provides an urban gradient of pollution [21], eventually helpful to identify the areas most affected by pollution, but does not guarantee proper information about the site taken into consideration. Moreover, those devices are cumbersome, bulky and unaesthetic when placed next to artifacts, as originally designed for assessing human exposure to atmospheric pollutants.

An exciting novelty to support this approach is provided by the European Air Quality Directives and reports [8], [10] that established the possibility to use not ISO recommended sensors to obtain indicative measurements or in support of "objective estimation" for air quality assessment, as long as they comply with the quality objectives set for each pollutant.

In this scenario, the deployment of a wireless sensors network (WSN) monitoring system presents valuable pros, such as: architecture scalability,

capability to integrate multiple and heterogeneous sensors on a single small node and possibility to distribute a high number of wireless and low-cost measurement points in the exhibition areas or at Historic sites [6], [128]. Moreover in literature is discussed and validate the possibility to use low-cost commercial sensors according to data quality objective (DQOs) of the citied directives [43], [44], [129].

Furthermore, in the last year, the same approach used for a technology transfer from assessing human exposure to cultural heritage exposure is applied to evaluate Risk Analyses following the standard recommendations [130]. Andretta et al. in particular, proposed "a new environmental risk assessment in indoor" cultural heritage protection based on a combination between the "Risk Index Methodology" and the "Dose-Response Methodology" [131]. In this research, we propose to evaluate a "Risk Index" for outdoor artifact or monument, where DOQs provide the upper bound limits for the single pollutant.

As above mentioned, recent studies showed how new instrumentations are developed to quantify the risk of cultural heritage about pollution. So we have realized and applied a complete solution, integrating sensors for environmental parameters (temperature and relative humidity), sensors for pollutant concentrations detection (SO_2, NO_x) and sensors for tilt and vibration detection [132], [133] tested in the site of so-called "Minerva Medica Temple." The device is expected to fuse the benefits of different non-integrated solutions recently proposed [40], [41], [98].

The aim of this work is monitoring effects of different factors affecting the "Minerva Medica Temple," an archeological site in Rome. In particular, we focus on: (i) the seasonal thermal variations on the structure; (ii) the contamination due to by local traffic regarding gaseous pollutant and (iii) the dynamic response of the structure to the "Roma- Giardinetti" tramway line.

In this research, we focus our attention principally on the description of the setup of WENDY. We also describe the software architecture and the Risk Analysis theory. Results of the research are presented and discussed.

MATERIALS AND METHODS

Firmware

WENDY firmware is realized with a bottom-up strategy and it is based on two external interrupts, one triggered by ds1337 RTC and one generated by BNO055. Figure 12 shows the measurement firmware flowchart with highlighted the most important functions.

The first interrupt (Alarm1) is set every minute. When entering the interrupt routine, the microcontroller firstly reads the Temperature (T in °C) value, relative humidity (RH in %) value and NO, NO_2, SO_2 (ppb) concentrations.

The second interrupt (Motion) is used to acquire data provided by the BNO055 when vibrations exceed a fixed threshold in term of acceleration.

It stores all data before in the internal EEPROM and then into an external SD memory card (to reduce the power supply consumption).

The MIMU is set with a cut-off frequency at 250 Hz and an acceleration range of ±2 g with a threshold of 3.91 mg as LSB and 996 mg as MSB. The value is chosen based on the UNI 9916 recommendation [120] as it will be explained in the following section. Both interrupts help to reduce the power consumption of battery power supply concerning a polling routine as, after the reading, sensors are switched off or put in safe-mode and the microcontroller enters the "sleep mode.". For the complete code, see Appendix A - Code.

All acquired data are analyzed in post-processing via MATLAB. In particular, for the data collected in "Timer Interrupt" stage, it is calculated the moving averages of the outputs, with a one-hour step and an 8-hour window (8h-Average). For data collected during the "Vibration Interrupt," the frequency and the velocity of vibration are evaluated and compared with the recommended values. To convert the data of gas sensors, we used the formula (Equation 2) provided by ISO 37120 [134]

$$\mu g / m^3 = \frac{(concentration) \cdot (12.187) \cdot (M)}{(273.15 + t)} \quad (2)$$

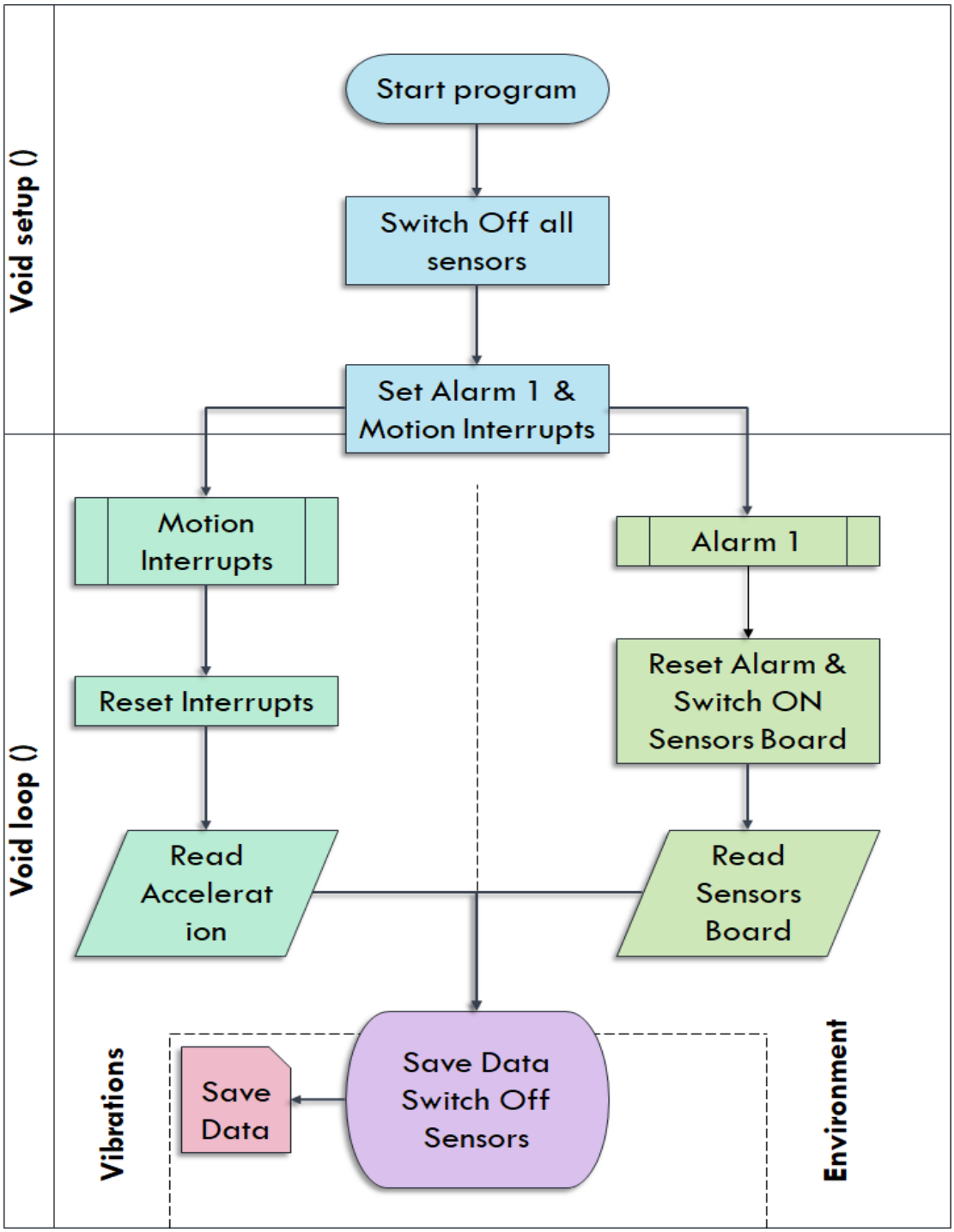

Figure 12 Measurement flow chart which highlighted the different states: the "void main ()," the "void loop ()" with the two internal interrupts: Motion and Alarm1.

Where M is the molecular weight of the gaseous pollutant, *concentration* is the gaseous pollutant concentration expressed in ppm and *t* the temperature expressed in °C.

Risk Analysis

Over the last year, many studies [23], [52] have provided to increase the knowledge about the kinetics and mechanisms of interactions environment-artworks and the impact of the climate changes on cultural heritage.

As discussed in the first sections, the application of mathematical models which integrate the data of active institutional samplers currently it is used to analyze the erosion/corrosion rate of the materials; they are based on the empirical Lipfert's formula and its variants [25], [135], [136]. An example is shown in Equation 3 below [137].

$$R = 3.1 + 0.01t\left(85 + 0.59Rh_{60}\left[SO_2\right] + 7.8Rh_{60}\left[HNO_3\right] + 5.4Rain\left[H^+\right] + 2.58PM_{10}\right) \quad (3)$$

R (expressed in μm) is the loss of mass due to corrosion, *t* (in years) is the time, the nitrogen oxides were indirectly considered to measure the HNO_3 (in $mg \cdot m^{-3}$), to start from the temperature values T (°C), relative humidity RH lower then 60%, NO_x and O_3 ($mg \cdot m^{-3}$). Even if these formulas correlate some pollutants, such as PM_{10}, SO_2, HNO_3 or acid rain amount, tend to underestimate the phenomenon and, do not have an overall solution because they are valid only for single material [52], [91], [138]; also this kind of model does not respond to any regulatory.

Fortunately, recent studies [139]–[141], have proposed a new approach to analyzing the cultural heritage's problems of protection and preservation and they are based on the risk management techniques, which is instead supported by the international standard regulatory [130].

Due to the success of risk assessment in many and heterogeneous areas (e.g., risk assessment of industrial systems or workplaces; environmental and ecological risk assessment; security and defense; economic and investment analysis; an objective and universal definition of risk is yet to be established [108], [142].

Currently, two definitions of Risk finds full application:

(1) The Risk (R) is the product of the Vulnerability (V) (the monument/artwork) for the Dangerous Effect (DE) (in our case the local environment).

(2) The Risk (R) can be seen as a measurement of the combined likelihood of occurrence of a Dangerous Event and its potential consequences.

In a recent study, Andretta [143] proposed a survey of different definitions of Risk, including a statistical approach to defining the risk assessment. This definition could be resumed as:

(3) "The risk R for a Targets of Interest $\{T_i\}$, due to an Anomalous State ST_a of the System S, which produces a Damage D of Magnitude M_d, is given by the probability $P(E_a)$ of an Adverse Effect on $\{T_i\}$ caused by the Damage D."

$$Risk\ R\ =\ \mathrm{P}\left(E_a\right) \tag{4}$$

Under the hypothesis of a well-defined *risk scenario* where the *Adverse* effects $\{E_a\}$ manifest on the targets of interest $\{T_i\}$ it is possible to rewrite Equation 4 as:

$$Risk\ R\ =\ \mathrm{P}\left(E_a\right) = P\left(E_a, M_d\right) \tag{5}$$

In this way, the causal relationship between the damage of magnitude Md and the adverse effect E_a is emphasized. In particular $P(E_a, M_d)$ is calculated over the set of all the ST_a that causes damage of magnitude M_d.

The second term of the relation, thanks to the so-called "general properties of unconditional and conditional probabilities" could be rewritten as:

$$Risk\ R\ =\ \mathrm{P}\left(E_a\right) = P\left(E_a, M_d\right) = P\left(E_a \mid M_d\right) \times P\left(M_d\right) \tag{6}$$

$P(M_d)$ represents the unconditional probability that the system S produces a source of risk of magnitude Md and $P(E_a|M_d)$ is the conditional probability due to M_d.

This new concept of Risk represents a turning-point in the risk analysis applied to the cultural heritage.

As known, environmental parameters affect cultural heritage in different ways. These hazards can compromise the stability of buildings and monuments, alter or destroy the characteristics of materials. For these reasons, the necessity to provide a risk assessment, in the short and long-term, for cultural heritage is a necessity for both academic and policy.

In cultural heritage, where existing a practical difficulty in establishing a representation of all components that act the during erosion/corrosion process, conducting a risk analysis through a probabilistic quantification of hazard can be considered as a helpful tool.

If we contextualize the third definition in the cultural heritage field, we have that: the *target* is an artifact or a monument and the *anomalous states* are the parameters that involving the deterioration of objects (*adverse effect*) with a certain intensity (M_d), while the system S is represented by road traffic or visitors inside a museum.

Furthermore, as defined in the recommendations of international certification organization ISO 30000 and ISO 30100 [130], [144], this work setting falls into a "*Relative Risk Assessment Methodology*" and doesn't require an exact knowledge of the probability function of Equation 6 but it is sufficient that the adverse effect could be defined with an S-shaped function (such as Probit or Logit models, or Dose-Response Curve,).

Risk Index

Pr (%)	*Rate*	*Range of tolerance*					
		0	*1*	*2*	*3*	*4*	*5*
0 ≤ Pr ≤ 20	**1**	0	1	2	3	4	5
20 < Pr ≤ 40	**2**	0	2	4	6	8	10
40 < Pr ≤ 60	**3**	0	3	6	9	12	15
60 < Pr ≤ 80	**4**	0	4	8	12	16	20
80 < Pr ≤ 100	**5**	0	5	10	15	20	25

Figure 13 The green cells represent good values (1); blue, grey and red respectively: acceptable (2), weak acceptable (3) and severe (4) values.

Moreover, the solution of Equation 6 is the numerical score called RI_x that represents the risk of a possible hostile result (Adverse Effect) which can be produced by abnormal values Md of the precise microclimatic variable x.

In this study, we obtain the RI_{tot} (total risk index) as the sum of the single Risk Index associated with the parameter under investigation. In particular, the microclimatic parameters set is chosen as follow:

- Temperature daily variation (ΔT);
- Relative Humidity daily variation (ΔRH);
- NO_x concentration;
- SO_2 concentration;
- vibration (p.p.v).

Both relative and total risk indexes are estimated realizing a probability matrix, as required by ISO 31000 [130].

The relative risk index RI_i for the i-th compound is calculated as the product between the level of frequency, associated with the percent probability that an *adverse effect* occurs and the range of tolerance of the *adverse effect*, in term of magnitude; if the combination frequencies/magnitudes yield different RI values,

it is considered the maximum one. M_d represents the difference between the threshold values and observed data related to the reference norms. The obtained matrix is portioned into four no-dimensional levels (1 to 4) as shown in Figure 13.

The total risk index RI_{TOT} is given by the sum of the output rank of all relative matrixes, it represents the synthetic and global index of the environment around the monument or artifact.

The five ranges, reported in Table 4 Deterioration level for the five chosen parameters, are settled as equipartition of the tolerance range. Mainly, we study the effects on the T_i concerning Amount (Time × Concentration) of the pollutant and the maximum level for each parameter is chosen equal to the maximum level required by recommendations. In particular for gas pollutant is used the "WHO Air quality guidelines for particulate matter, ozone, nitrogen dioxide and sulfur dioxide: global update 2005 - summary of risk assessment" for human health monitoring [119] and the UNI 9916 recommendation to evaluating vibration effects on structures of archaeological and historical value (cultural heritage) [120]. For the daily temperature and relative humidity fluctuating, the range is chosen in function of the UNI 10925:2001 and UNI 10829:1999 [90], [121].

Table 4 Deterioration level for the five chosen parameters

Deterioration level						
Parameters	**Range of tolerance**					
	Range 0	Range 1	Range 2	Range 3	Range 4	Range 5
ΔT (°C)	≤ 4	4÷6	6÷8	8÷10	10÷12	≥ 12
ΔRH (%)	≤ 15	15÷20	20÷25	25÷30	30÷35	≥ 35
SO_2 ($\mu g/m^3$)	≤ 100	100÷200	200÷300	300÷400	400÷500	≥ 500
NO_x ($\mu g/m^3$)	≤ 40	40÷80	80÷120	120÷160	160÷200	≥ 200
p.p.v. (mm/s)	≤ 1	1÷2	2÷3	3÷4	4÷5	≥ 5

Equation 7 explicates the Risk Index, it is calculated respect to the five chosen parameters and becomes as follows:

$$RI_{tot} = \sum_i RI_i = RI_{\Delta T} + RI_{\Delta RH} + RI_{SO_2} + RI_{NO_x} + RI_{ppv} \quad (7)$$

RI_{tot} is characterized by four levels: $RI_{tot} = 5$ (good), $RI_{tot} =]5,10]$ (acceptable), $RI_{tot} =]10,15]$ (weak acceptable) and $RI_{tot} =]15,20]$ (severe), for a total range $9 \leq RI_{tot} \leq 20$.

All acquired data are analyzed in post-processing via MATLAB. In particular, for the daily ΔT and ΔRH, we evaluate the maximum excursion for each day, for SO_2 and NO_x we evaluate the percent distribution in the full observation window and for p.p.v the percent distribution in the full observation window relative to the amount of event associated to a vibration that exceeds the chosen threshold. According to UNI 9916, the monitored vibrations (induced by trains, tram and bus) fall into the classification of "occasional short-term vibrations."

Application site

The test of the device has been conducted at the so-called "Minerva Medica Temple."

"Minerva Medica" is an Ancient Roman temple, nowadays nestled between Roma Termini railway station and the "Roma-Giardinetti" tramway line. The structure presents a decagonal plant and nine niches around the structures. We chose the third from the entrance and moving right. The chosen point is at 0.35 m from ground level; it is compliant with UNI 9916 [120] that indicates 0.50 meters as the maximum value for measurement at the ground. The measurement campaigns carried out between the 2017 and 2018 over two different periods (September-December '17 and March-July '18) due to the closure of the archaeological site.

Additionally, due to the impossibility to a Network Access and to place a personal computer in the archeological site, we decide to waive the wireless communication and use only the SD data memory

Figure 14 Minerva Medica Temple

Figure 15 Placing of the measurement system at the third niche of Minerva Medica Temple at 35 cm.

RESULTS AND DISCUSSION

Figure 16 a) and b) report the magnitude of ΔT (°C) and ΔRH (%) for the first period (September-December), in function of the tolerance range. The different levels are highlighted in the background: range 0 in green, range 1 in light-blue, rage 2 in yellow, range 3 in grey, range 4 in pink and range 5 in violet.

Applying the definition of RI is possible to evaluate for temperature and relative humidity $RI_{\Delta T} = 1$ and $RI_{\Delta RH} = 2$ due to: a 90% of ΔT value inside range 0 and a 40% of ΔRH value inside the range 1.

Figure 16 c) and Figure 16 d) report the outline of SO_2 and NO_x (μg/m^3), while Figure 16 e) shows the p.p.v values for each day. For the three above mentioned figures we use the same color scheme of Figures 16 a) and 16 b). Furthermore, following the same procedure for the other pollutant results that $RI_{SO2} = 1$ due to the 85% of values is inside Range 0, $RI_{NOx} = 2$ due to the 65% of values are in Range 1 and $RI_{ppv} = 3$ with the 90% of values in Range 2.

Figure 17 a) and Figure 17 b) report the magnitude of ΔT (°C) and ΔRH (%) for the second period (March-July), in function of the tolerance range. The different levels are always highlighted with the just cited color scheme: range 0 in green, range 1 in light-blue, rage 2 in yellow, range 3 in grey, range 4 in pink and range 5 in violet.

In the second monitoring window $RI_{\Delta T} = 1$ and $RI_{\Delta RH} = 1$ due to: a 70% of ΔT value inside range 0 and a 70% of ΔRH value inside the range 0.

Figure 17 c) and Figure 17 d) report the outline of SO_2 and NO_x (μg/m3), while Figure 17 e) shows the p.p.v values for each day. For the three above mentioned figures, we use the same color scheme of Figures 17 a) and 17 b).

Furthermore, following the same procedure for the other pollutant results that $RI_{SO2} = 1$ due to the 95% of values is inside Range 0, $RI_{NOx} = 2$ due to the 76% of values are in Range 1 and $RI_{ppv} = 3$ with the 90% of values in Range 2.

Figure 18 shows the results of RI_{tot}. It shows the histograms of the synthetic risk index, given by the sum of all the Rix. The results of this kind of methodologies show how the monument is globally in the acceptable range but at the same time highlight which is the parameters that profoundly influence the conservation of the structure.

$$\begin{aligned} &a) \quad RI_{tot} = \sum_i RI_i = RI_{\Delta T} + RI_{\Delta RH} + RI_{SO_2} + RI_{NO_x} + RI_{ppv} = 1+2+1+2+3 = 9 \\ &b) \quad RI_{tot} = \sum_i RI_i = RI_{\Delta T} + RI_{\Delta RH} + RI_{SO_2} + RI_{NO_x} + RI_{ppv} = 1+1+1+2+3 = 8 \end{aligned} \tag{8}$$

Equation 8 a) reports the RI_{tot} for the first part of monitoring, while Equation 8 b) reports the RI_{tot} for the second part of monitoring. Both values lower than ten, represent an *acceptable* value of RI.

The dependence of vibration showed in other paper [100], [145], is however highlighted with this method. Also, even if RI_{ppv} is in the weak accepted range, the maximum value is lower than the recommended value. Moreover, the increase in term of magnitude in June is due to the movement of the scaffoldings in site during the restoration activities.

a)

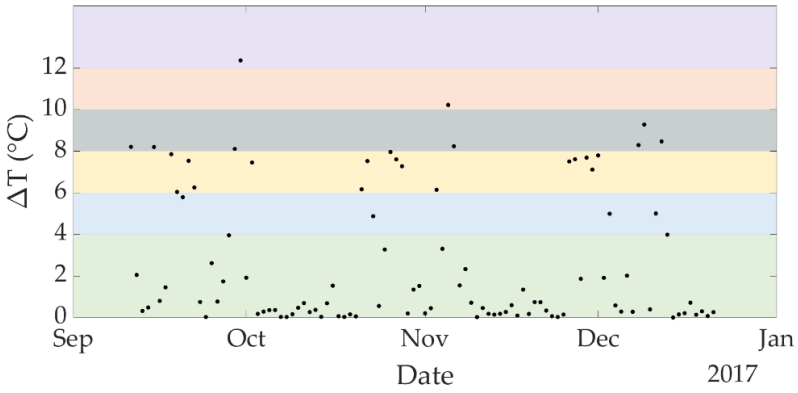

$RI_{\Delta T} = 1$

b)

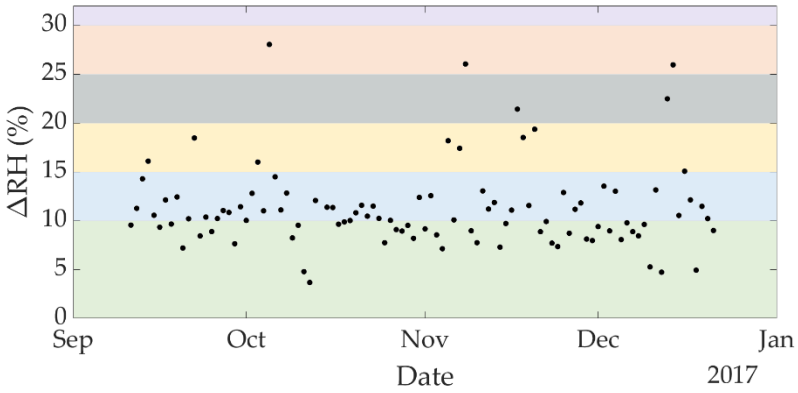

$RI_{\Delta RH\%} = 2$

c)

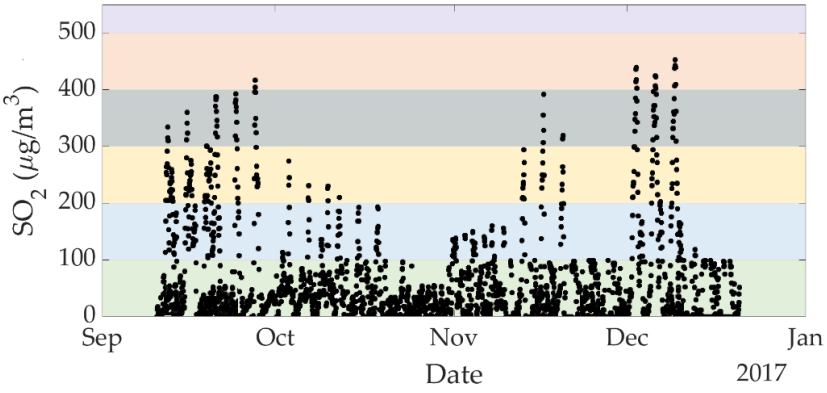

$RI_{SO2} = 1$

Figure 16 - Range 0 in green, Range 1 in light-blue, Rage 2 in yellow, Range 3 in grey, Range 4 in pink and Range 5 in violet.

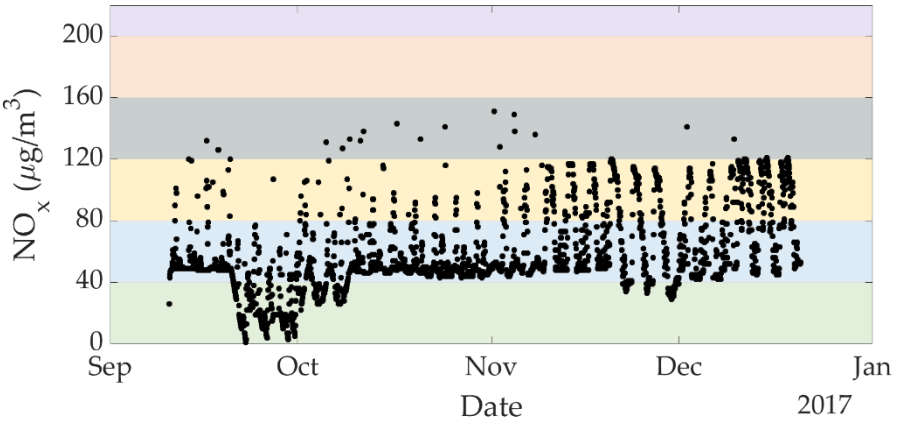

d)

$RI_{NOX} = 2$

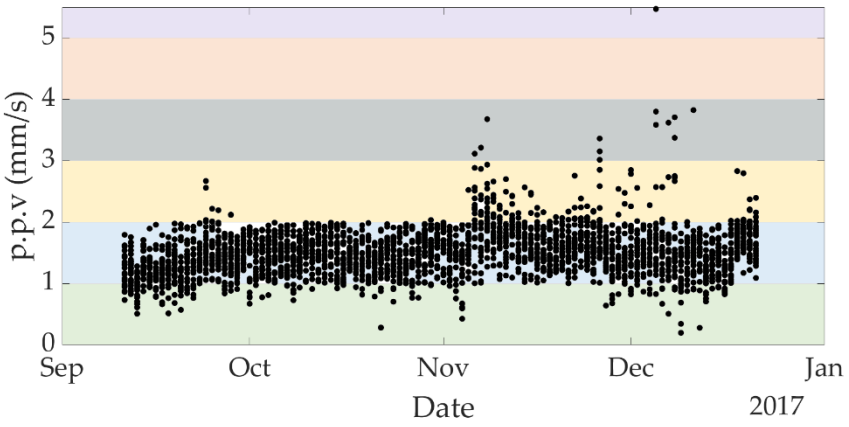

e)

$RI_{PPV} = 2$

Figure 16 The magnitude of the five chosen parameters (ΔT, ΔRH, SO_2, NO_x and p.p.v.) in function of the different range. In all graphs, we have highlighted the different ranges with different colors. Range 0 in green, Range 1 in light-blue, Rage 2 in yellow, Range 3 in grey, Range 4 in pink and Range 5 in violet.

a)

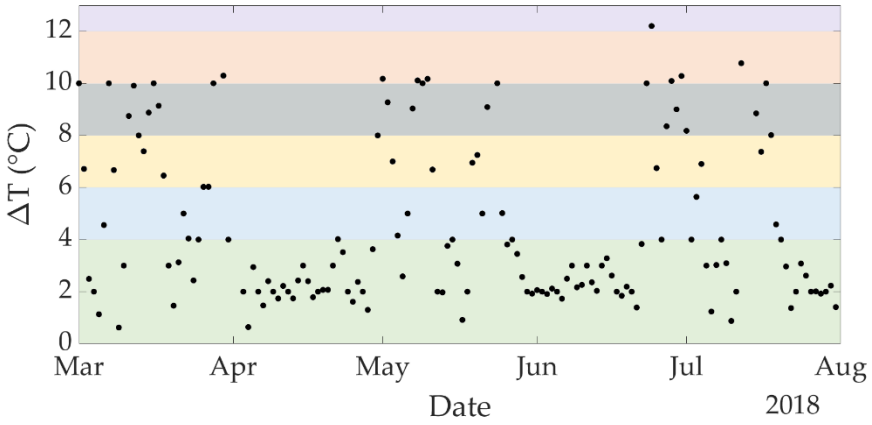

$RI_{\Delta T} = 1$

b)

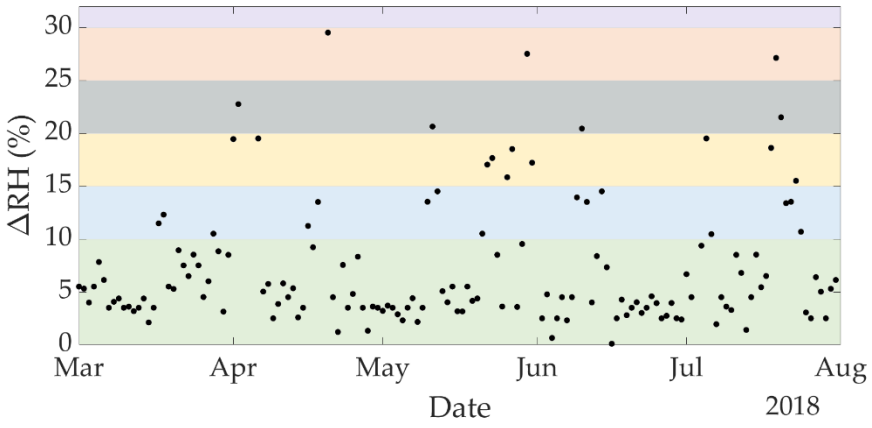

$RI_{\Delta T} = 1$

c)

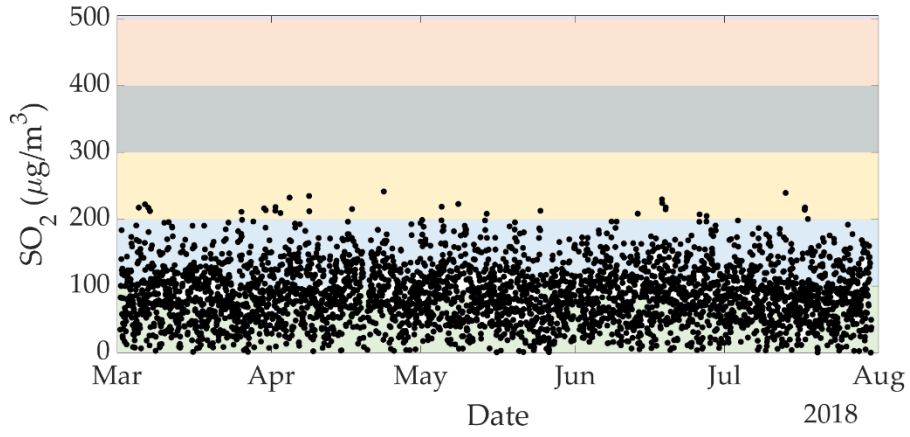

$RI_{SO2} = 1$

Figure 17 - Range 0 in green, Range 1 in light-blue, Rage 2 in yellow, Range 3 in grey, Range 4 in pink and Range 5 in violet

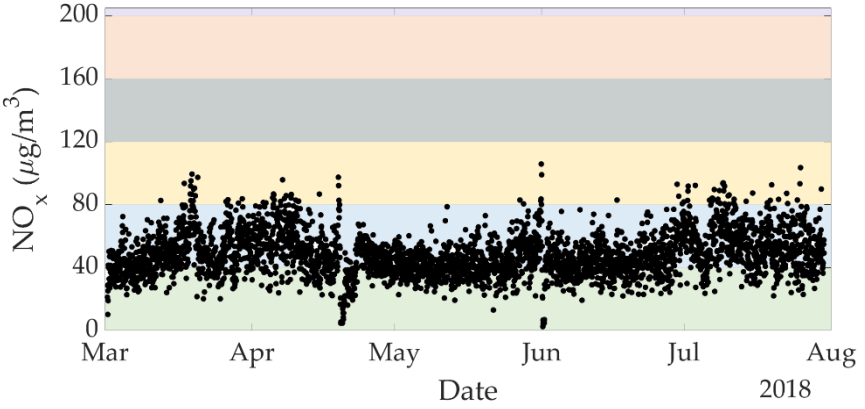

d)

$RI_{NOX} = 2$

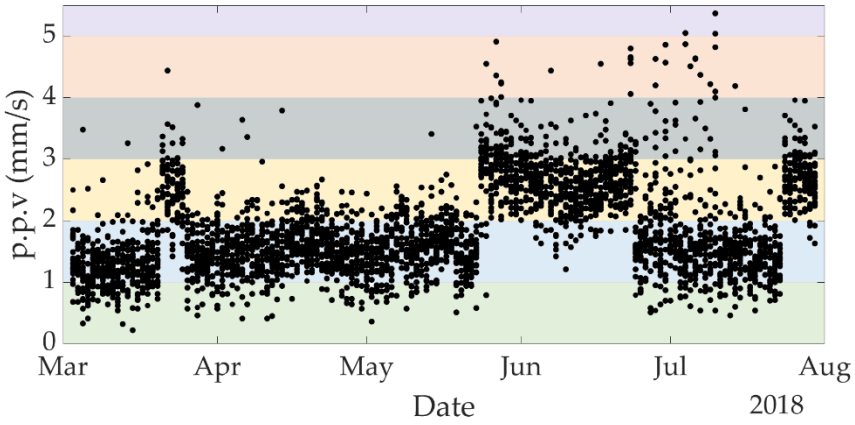

e)

$RI_{ppv} = 2$

Figure 17 The magnitude of the five chosen parameters (ΔT, ΔRH, SO_2, NO_x and p.p.v.) in function of the different range. In all graphs, we have highlighted the different ranges with different colors. Range 0 in green, Range 1 in light-blue, Rage 2 in yellow, Range 3 in grey, Range 4 in pink and Range 5 in violet.

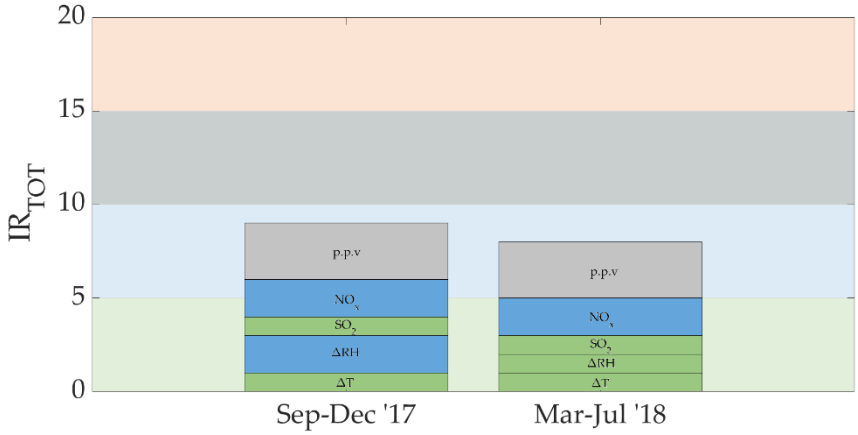

Figure 18 IRtot for the two monitorings

CONCLUSION

In the present work, we described a system for monitoring the effects of thermal variations, trolley vibrations and traffic pollution on an ancient Roman structure. The advantages of the system are (i) integration of multiple and heterogeneous sensors on a single node and (ii) a lower cost about to traditional instrumentation. In addition, the proposed algorithm permits to evaluate a *Risk Index* associated to a monument using the same limitation (in term of magnitude limit) for the human health monitoring but using a different approach: the cumulative dose-response independents to the hourly threshold provided by recommendation (human doses).

Summary and General Discussion

This work was divided into three sections.

Part 1 contains a survey about the state of art of the technology currently applied in the cultural heritage analysis. The review covered the last ten years until 2012; it is possible to see extensive use of dosimeters or passive samplers in general. After this date, it is possible to see an increase of sensors-based samplers. Some modern functional evaluation protocols, aimed at the quantitative evaluation of physical parameters and environmental diagnosis were also discussed. Special attention was paid to the pollutant common analyzed that mostly interacts with materials. At last some considerations about the usefulness of low-cost solution for the monitoring of the environment around the cultural heritage objects/monuments are proposed. This review section represents the bibliographic work conducted during the first year.

Part 2 concerns the design of the device and the experimental setup involving tilt/vibration, temperature, relative humidity and gaseous concentration analysis. This work was aimed to investigate the accuracy of the low cost towards of certified and calibrated sensors.

The analysis conducted during the second year investigated the output of BNO055 in tilt and shock detection regarding stability and accuracy, showing an SD of 0.4° in tilt detection and an nRMSE lover than 20% and 52% for sin and sinc signal stimulation. Additionally, the accuracy of first peak detection was evaluated lower than 1%. The gas concentration shows a compatible output with certified network analyzer detecting the same hourly peaks. Hygro-thermal sensors show an RMSE of 0.11 °C and 0.18% respectively.

Part 3 concerns the application of the realized device in the real case, namely the so-called "Minerva Medica Temple" in Rome during the third year. Additionally, a Risk assessment index to quantify the degradation effect on the

monument has been presented. According to the ISO recommendation, it is based on a "Relative Risk Assessment Methodology.

The goal of this research is to evaluate the effects of the different parameters affecting the archeological site so-called "Minerva Medica Temple," in Rome. In particular, we focus on: (i) the contamination due to by local traffic regarding gaseous pollutant, (ii) the seasonal thermal variations on the structure and (iii) the dynamic response of the structure to the "Roma- Giardinetti" tramway line.

Currently, we are improving the performance of the WENDY device, adding sensors for O_3, PM_{tot} concentration and light intensity. At the moment, in order to ensure the wireless communication, we realize a master-unit based on a RaspbarryPi 3B+ model→ In this way, using a microcomputer directly, we can avoid the MatLab post-processing activities. The aim for the future is to realize more slave-units, increasing the knowledge of the environment in an archeological site consequently and better improve the Risk Index proposed.

Appendix

APPENDIX A - CODE

```
/*Code for Minerva Medica
*/
//library
#include <DS1337.h> //RTC
#include <Wire.h> // I2C
#include <SPI.h> //SPI
#include <SD.h> //memory card
#include <Sensor.h> //mathematical function; and EEPROM routine
#include <BME280.h> // T,RH,P sensor
#include "NAxisMotion.h" //motion sensor and buffer interrupt;

//rtc local variable
DS1337 rtc;
volatile boolean alarm = false;
Date dt;

//bme280 local variable
BME280 bme;

//sd-card local variable
const int chipSelect = 4;

// variabili per BMO055
NAxisMotion mySensor;   //Object that for the sensor
```

```
bool intDetected = false;          //Flag to indicate if an interrupt was detected
int threshold = 2;
int duration = 1;
bool anyMotion = true; //To know which interrupt was triggered
bool updateSensorData = true;

//variabili gas
#define TARGET_GAS 0x02

void setup() {
    // Open serial communications and wait for port to open:
    Serial.begin(115200);
    I2C.begin();
    while (!Serial) {
    // wait for serial port to connect. Needed for native USB port only
    }

Serial.print("Initializing SD card...");

    // see if the card is present and can be initialized:
    if (!SD.begin(chipSelect)) {
    return;
    }

    rtc.init();
    rtc.setTickMode(DS1337_NO_TICKS);
    rtc.clearFlags();
```

```
// set date and time
rtc.setDate(17, 9, 13);
rtc.setTime(7, 30);
rtc.clearAlarm();
rtc.setAlarm(00);
// alarm on exact match
rtc.setAlarmMode(DS1337_ALARM_ON_SECOND);
// enable
rtc.enableAlarm();

// attach interrupt
pinMode(2, INPUT);
attachInterrupt(0, onAlarm, FALLING);

bool status;

//default settings
status = bme.begin();

mySensor.initSensor();
mySensor.setOperationMode(OPERATION_MODE_ACCONLY);
mySensor.setUpdateMode(MANUAL);
pinMode(3, INPUT);
attachInterrupt(1, motionISR, RISING);  //Attach the interrupt to the Interrupt Service Routine for a Rising Edge. Change the interrupt pin depending on the board
```

```
        mySensor.writeAccelConfig(ACCEL_RANGE_2G,  ACCEL_BW_250HZ,
ACCEL_NORMAL);
    mySensor.updateAccelConfig();
    mySensor.setPowerMode(POWER_MODE_LOWPOWER);

    updateSensorData = true;

    mySensor.enableSlowNoMotion(threshold, duration, SLOW_MOTION);
    anyMotion = false;
    mySensor.accelInterrupts(ENABLE, ENABLE, ENABLE);
    }

    void loop() {

    // make a string for assembling the data to log:
    if (alarm) {
    // clear alarm
    rtc.clearAlarm();
    alarm = false;
    // print current date and time

    // open the file. note that only one file can be open at a time,
    // so you have to close this one before opening another.
    File dataFile = SD.open("datalog.txt", FILE_WRITE);
    // if the file is available, write to it:
     if (dataFile) {
    dt = rtc.getDate();
```

```
dataFile.print(dt.getDateString());
dataFile.print(" ");
dataFile.print(dt.getTimeString());
dataFile.print('\t');
dataFile.print(bme.readTemperature());
dataFile.print('\t');
dataFile.print(bme.readHumidity());
dataFile.print('\t');
Wire.beginTransmission(TARGET_GAS);
Wire.requestFrom(TARGET_GAS, 2); // request 1 byte
// from slave device
while (Wire.available() > 0) {
int i = Wire.read();
int j = Wire.read();
int h = Wire.read();
int t = Wire.read();
int w = Wire.read();
int r = Wire.read();

dataFile.print(word(i, j) / .342F);
dataFile.print('\t');
dataFile.print(word(h, t) / .372F);
dataFile.print('\t');
dataFile.println(word(w, r) / .197F);
}
Wire.endTransmission();
dataFile.close();
```

```
    // print to the serial port too:
    }
    // if the file isn't open, pop up an error:
    else {
    Serial.println("error opening datalog.txt");
    }
    }

    if (intDetected) {
    intDetected = false;
    mySensor.resetInterrupt();          //Reset the interrupt line
    mySensor.disableAnyMotion();        //Disable the Any motion interrupt
    mySensor.enableSlowNoMotion(threshold,    duration,    SLOW_MOTION);
//Enable the No motion interrupt (can also use the Slow motion instead)
    anyMotion = false;
    File dataFile1 = SD.open("datalog1.txt", FILE_WRITE);
    dt = rtc.getDate();
    dataFile1.print(dt.getDateString());
    dataFile1.print(" ");
    dataFile1.print(dt.getTimeString());
    dataFile1.print('\t');
    // if the file is available, write to it:
     if (dataFile1) {
    mySensor.updateAccel();
    dataFile1.print(mySensor.readAccelX());
    dataFile1.print('\t');
    dataFile1.print(mySensor.readAccelY());
```

```
dataFile1.print('\t');
dataFile1.print(mySensor.readAccelZ());
dataFile1.print('\n');
bool updateSensorData = true;
dataFile1.close();
// print to the serial port too:

}
// if the file isn't open, pop up an error:
else {
}
}
void onAlarm() {
noInterrupts();
alarm = true;
interrupts();
}
void motionISR()
{
noInterrupts();
intDetected = true;
interrupts();

}
```

APPENDIX B – OTHER RESEARCH

During the Ph.D. I have conducted other researches principally in collaboration with the Department of Information Engineering, Electronics and Telecommunication (DIET) of Sapienza University of Rome.

The collaboration with the laboratory of Electromagnetic Field, directed by prof. F. Frezza, has produced a work entitled "Tag recognition: A new methodology for the structural monitoring of cultural heritage." In this work, as described in the abstract "a new methodology for measuring the cracking in the field of Structural Health Monitoring (SHM) of cultural heritage, is presented. The minimum invasiveness of this methodology permits to preserve the aesthetic appearance, a fundamental requirement in the monitoring of cultural heritage. The core of the acquisition system is composed by two small adhesive tags to be attached on the artwork surface and a high-resolution camera acquires images of the tags. The relative distance between the optical tags is determined using advanced least-squares fitting of quadratic curves and surfaces algorithms for the objective function. Here, in order to find the best configuration for determining the fitting parameters, useful for the SHM, the bi-dimensional Gaussian as an objective function has been taken into account heritage applications. We ran a simulation for tuning fitting algorithm parameters. Then we validated the methodology through an experimental session. From the real measurements, in a controlled environment, it was found that with the proposed measurement system it was possible to determine displacements of the order of ten micrometers at a camera-tags distance of 25 cm and with a relative error lower than 3%."

The collaboration with the laboratory of Electric and Electronic Measurement, directed by prof. E. Piuzzi, has produced two works always related cultural heritage applications.

The first one entitled *Effect of Applied Pressure on Patch Resonator-Based Measurements of Moisture Level for Cultural Heritage Materials*, regards the "preliminary results of the variations of the reflection coefficient of a planar patch resonator placed in contact with cultural heritage stone materials in function of applied mechanical pressure. The general aim of the experimental project is to correlate the resonant frequency of the planar sensor, for the different pressures applied to the resonator, with the different levels of water content θv of the tested stone material. In fact, in previous works, it has been demonstrated that by placing a planar resonator in contact with the considered stone sample, it is possible to associate the resonant frequency of the resonator with the moisture content of the stone sample, through reflection scattering parameter measurements. In previous studies, however, the level of applied pressure is not standardized and controlled. An application of an external force could improve the repeatability and increase the detectability of the first resonance peak. The current study shows a negligible resonant frequency shift among measurements with different applied pressures at the same water content θv level, but a significant change regarding Q factor. Moreover, applying an external force on the patch, the first resonance peak can be identified more easily, thanks to an increase in the Q factor."

The second one is entitled *Compensating for Bulk Density Effect in Permittivity-Based Moisture Content Measurements on Cultural Heritage Materials*. It could be summarized as "Dielectric permittivity-based measurement techniques are establishing themselves as attractive solutions for assessing moisture content of Cultural Heritage structures. The relative simplicity of the measurement principle and the inherent adaptability to diverse operating conditions are two of the most notable features of these techniques. In spite of these specific advantages, however, there are still some aspects that hinder the widespread use

of permittivity-based moisture content measurement systems and make their standardization difficult. In particular, the bulk density of the sample under test may affect the estimation of permittivity, thus possibly leading to inaccurate moisture content measurements. As a result, the measurement system should be re-calibrated even when the same type of material is being investigated (e.g., two samples of the same type of stone, but extracted from different places). To circumvent this problem and to fully exploit the potential of permittivity-based moisture content measurements, in this work, a strategy for compensating for the effect of bulk density is addressed. In order to verify the suitability of this strategy, moisture content measurements were carried out on samples of two type of stones that are typically used in Cultural Heritage structures, namely gentile stone and red-clay brick."

Other two works, outside the measurements in cultural heritage field, regard biomechanical applications. A short abstract is reported for the first one entitled: *Tetrapolar Low-Cost Systems for Thoracic Impedance Plethysmography*. "Bioelectrical impedance analysis applied to the pneumographic investigation is a technique for monitoring the respiratory activity through the measurement of variations in the trans-thoracic electrical impedance. In this paper, a low-cost reconfigurable measurement system is presented. The system is based on a 4-electrode volt-amperometric technique and a network of inertial sensors for correction of arms motion artifacts. The trans-thoracic impedance was acquired via an ad- hoc programmed LabVIEW software. A correction algorithm, based on the correlation between the acquired signal and the motion artifact, was proposed. A preliminary metrological assessment of the system was performed to evaluate the accuracy and sensitivity to patient breath monitoring. Results show high accuracy in a 100 Ω range of measurement. The proposed algorithm allows for

the estimation of the thoracic impedance with a maximum error of 30% and to neglect the phase shift between the breath and the movement signals."

Similarly, we report an abstract of the second work entitled *Development and mechanical validation of an in vitro system for bone cell vibration loading.*

"Vibration loading, both low magnitude and high magnitude at high frequency, has been demonstrated to have an anabolic effect on bone cells. The study of the mechanotransduction, the process by which mechanical loadings are detected by cells and converted in the chemical signal, is made accessible through the use of in vitro loading system. The aim of an in vitro loading system is to recreate the forces acting in the cell microenvironment. The goal of this study was to develop and mechanically validate a vibration loading system able to engender sinusoidal vertical vibration at different combinations of magnitude (0.3 g, 1 g and 3 g) and frequency (30 Hz, 60 Hz and 90 Hz). A system like this can be therefore employed to study cell response to high and low magnitudes at high frequencies, thus providing a comprehensive evaluation of bone cell mechanotransduction. The mechanical validation that is the characterization of the right loading input to the system to obtain the desired stimulation on cell culture was performed in two different methods: open-loop and closed-loop mode. The results obtained in the open-loop mode showed good intra-day repeatability of the measurements with values of the index of dispersion always lower than 0.6%. While in the closed-loop mode a systematic search was implemented to reach the optimal amplitude stimulation. The vibration signals acquired on a long-term test following the systematic search showed good stability with an index of dispersion always lower than 1%. Following the mechanical validation, the system was used to stimulate osteoblast-like cells (Saos-2) with vibration loading of nine combinations of magnitude and frequency and the cell proliferation was studied 24h after the treatment by cell

counting. Our preliminary results showed that no alterations in the proliferation were induced by 90 Hz vibration loading. On the other hand, small modulations in the proliferation were reported for lower stimulation frequency, being statistically significant when using 0.3 g of amplitude at 30 Hz."

References

[1] S. Brienza, A. Galli, G. Anastasi, and P. Bruschi, "A Low-Cost Sensing System for Cooperative Air Quality Monitoring in Urban Areas," *Sensors*, vol. 15, no. 6, pp. 12242–12259, May 2015.

[2] F. Borghi *et al.*, "Miniaturized monitors for assessment of exposure to air pollutants: A review," *Int. J. Environ. Res. Public Health*, vol. 14, no. 8, 2017.

[3] Y. Xiang, Y. Tang, and W. Zhu, "Mobile sensor network noise reduction and recalibration using a Bayesian network," *Atmos. Meas. Tech.*, vol. 9, no. 2, pp. 347–357, Feb. 2016.

[4] P. Kumar *et al.*, "The rise of low-cost sensing for managing air pollution in cities.," *Environ. Int.*, vol. 75, pp. 199–205, Feb. 2015.

[5] N. Castell *et al.*, "Can commercial low-cost sensor platforms contribute to air quality monitoring and exposure estimates?," *Environ. Int.*, vol. 99, pp. 293–302, Feb. 2017.

[6] L. Morawska *et al.*, "Applications of low-cost sensing technologies for air quality monitoring and exposure assessment: How far have they gone?," *Environ. Int.*, vol. 116, no. February, pp. 286–299, 2018.

[7] P. S. Kanaroglou *et al.*, "Establishing an air pollution monitoring network for intra-urban population exposure assessment: A location-allocation approach," *Atmos. Environ.*, vol. 39, no. 13, pp. 2399–2409, Apr. 2005.

[8] EU, "Directive 2008/50/EC of the European Parliament and of the Council of 21 May 2008 on ambient air quality and cleaner air for Europe," 2008.

[9] M. S. Ragettli *et al.*, "Commuter exposure to ultrafine particles in different urban locations, transportation modes and routes," *Atmos. Environ.*, vol. 77, pp. 376–384, Oct. 2013.

[10] C. Guerreiro, A. Gonzalez Ortiz, F. de Leeuw, M. Viana, and J. Horalek, *Air quality in Europe — 2016 report*, no. 28. 2016.

[11] E. G. Snyder *et al.*, "The changing paradigm of air pollution monitoring.," *Environ. Sci. Technol.*, vol. 47, no. 20, pp. 11369–77, 2013.

[12] A. Proietti, L. Liparulo, F. Leccese, and M. Panella, "Shapes classification of dust deposition using fuzzy kernel-based approaches," *Measurement*, vol. 77, pp. 344–350, Jan. 2016.

[13] *Sensors and Actuators A: Physical*, no. v. p. 273.

[14] N. Castell *et al.*, "Mobile technologies and services for environmental monitoring: The Citi-Sense-MOB approach," *Urban Clim.*, vol. 14, pp. 370–

382, Dec. 2015.

[15] C. M. Grzywacz, *Monitoring for Gaseous Pollutants in Museum Environments*, First. Los Angeles: Getty Publications, 2006.

[16] H. Agbota, C. Young, and M. Strlič, "Pollution monitoring at heritage sites in developing and emerging economies," *Stud. Conserv.*, vol. 58, no. 2, pp. 129–144, 2013.

[17] "Model 43i SO2 Analyzer." [Online]. Available: https://www.thermofisher.com/order/catalog/product/43I.

[18] D. Saraga, S. Pateraki, A. Papadopoulos, C. Vasilakos, and T. Maggos, "Studying the indoor air quality in three non-residential environments of different use: A museum, a printery industry and an office," *Build. Environ.*, vol. 46, no. 11, pp. 2333–2341, Nov. 2011.

[19] R. S. Hamilton, H. Crabbe, S. Fitz, and T. Grøntoft, "Monitoring, Modelling and Mapping," in *The Effects of Air Pollution on Cultural Heritage*, R. Hamilton, V. Kucera, J. Tidblad, and J. Watt, Eds. Boston, MA: Springer US, 2009, pp. 29–51.

[20] D. De la Fuente, J. M. Vega, F. Viejo, I. Díaz, and M. Morcillo, "Mapping air pollution effects on atmospheric degradation of cultural heritage," *J. Cult. Herit.*, vol. 14, no. 2, pp. 138–145, 2013.

[21] D. de la Fuente, J. M. Vega, F. Viejo, I. Diaz, and M. Morcillo, "City scale assessment model for air pollution effects on the cultural heritage," *Atmos. Environ.*, vol. 45, no. 6, pp. 1242–1250, 2011.

[22] F. Karaca, "Mapping the corrosion impact of air pollution on the historical peninsula of Istanbul," *J. Cult. Herit.*, vol. 14, no. 2, pp. 129–137, 2013.

[23] A. De Marco, A. Screpanti, M. Mircea, A. Piersanti, C. Proietti, and M. F. Fornasier, "High resolution estimates of the corrosion risk for cultural heritage in Italy," *Environ. Pollut.*, vol. 226, pp. 260–267, 2017.

[24] F. Di Turo *et al.*, "Impacts of air pollution on cultural heritage corrosion at European level: What has been achieved and what are the future scenarios," *Environ. Pollut.*, vol. 218, pp. 586–594, 2016.

[25] M. Saba, E. E. Quiñones-Bolaños, and A. L. Barbosa López, "A review of the mathematical models used for simulation of calcareous stone deterioration in historical buildings," *Atmos. Environ.*, vol. 180, no. September 2017, pp. 156–166, 2018.

[26] L. Mašková, J. Smolík, and M. Ďurovič, "Characterization of indoor air quality in different archives – Possible implications for books and manuscripts," *Build. Environ.*, vol. 120, pp. 77–84, 2017.

[27] T. Grøntoft *et al.*, "Pollution monitoring by dosimetry and passive diffusion sampling for evaluation of environmental conditions for paintings in microclimate frames," *J. Cult. Herit.*, vol. 11, no. 4, pp. 411–419, 2010.

[28] A. Worobiec *et al.*, "Transport and deposition of airborne pollutants in exhibition areas located in historical buildings-study in Wawel Castle Museum in Cracow, Poland," *J. Cult. Herit.*, vol. 11, no. 3, pp. 354–359, 2010.

[29] M. Carminati, G. Ferrari, and M. Sampietro, "Emerging miniaturized technologies for airborne particulate matter pervasive monitoring," *Measurement*, vol. 101, pp. 250–256, Apr. 2017.

[30] F. Sciurpi, C. Carletti, G. Cellai, and L. Pierangioli, "Environmental monitoring and microclimatic control strategies in 'la Specola' museum of Florence," *Energy Build.*, vol. 95, pp. 190–201, 2015.

[31] J. Ferdyn-Grygierek, "Indoor environment quality in the museum building and its effect on heating and cooling demand," *Energy Build.*, vol. 85, pp. 32–44, 2014.

[32] F. Becherini, A. Bernardi, and E. Frassoldati, "Microclimate inside a semi-confined environment: Valuation of suitability for the conservation of heritage materials," *J. Cult. Herit.*, vol. 11, no. 4, pp. 471–476, 2010.

[33] H. Janssen and J. E. Christensen, "Hygrothermal optimisation of museum storage spaces," *Energy Build.*, vol. 56, pp. 169–178, 2013.

[34] J. Ferdyn-Grygierek and A. Baranowski, "Internal environment in the museum building—Assessment and improvement of air exchange and its impact on energy demand for heating," *Energy Build.*, vol. 92, pp. 45–54, Apr. 2015.

[35] J. Ferdyn-Grygierek, "Monitoring of indoor air parameters in large museum exhibition halls with and without air-conditioning systems," *Build. Environ.*, vol. 107, pp. 113–126, Oct. 2016.

[36] B. Krupinska *et al.*, "Assessment of the air quality (NO2, SO2, O3 and particulate matter) in the Plantin-Moretus Museum/Print Room in Antwerp, Belgium, in different seasons of the year," *Microchem. J.*, vol. 102, no. 2, pp. 49–53, 2012.

[37] B. Krupinska, R. Van Grieken, and K. De Wael, "Air quality monitoring in a museum for preventive conservation: Results of a three-year study in the Plantin-Moretus Museum in Antwerp, Belgium," *Microchem. J.*, vol. 110, pp. 350–360, 2013.

[38] R. H. M. Godoi *et al.*, "Indoor air quality of a museum in a subtropical climate: The Oscar Niemeyer museum in Curitiba, Brazil," *Sci. Total*

Environ., vol. 452–453, pp. 314–320, 2013.

[39] F. Lamonaca, G. Pizzuti, N. Arcuri, A. M. Palermo, and R. Morello, "Monitoring of environmental parameters and pollution by fungal spores in the National Gallery of Cosenza: A case of study," *Measurement*, vol. 47, no. 1, pp. 1001–1007, Jan. 2014.

[40] A. Proietti, M. Panella, F. Leccese, and E. Svezia, "Dust detection and analysis in museum environment based on pattern recognition," *Measurement*, vol. 66, pp. 62–72, 2015.

[41] M. I. Mead *et al.*, "The use of electrochemical sensors for monitoring urban air quality in low-cost, high-density networks," *Atmos. Environ.*, vol. 70, pp. 186–203, May 2013.

[42] F.-J. Diego, B. Esteban, and P. Merello, "Design of a Hybrid (Wired/Wireless) Acquisition Data System for Monitoring of Cultural Heritage Physical Parameters in Smart Cities," *Sensors*, vol. 15, no. 4, pp. 7246–7266, Mar. 2015.

[43] L. Spinelle, M. Gerboles, M. G. Villani, M. Aleixandre, and F. Bonavitacola, "Field calibration of a cluster of low-cost available sensors for air quality monitoring. Part A: Ozone and nitrogen dioxide," *Sensors Actuators B Chem.*, vol. 215, pp. 249–257, Aug. 2015.

[44] L. Spinelle, M. Gerboles, M. G. Villani, M. Aleixandre, and F. Bonavitacola, "Field calibration of a cluster of low-cost commercially available sensors for air quality monitoring. Part B: NO, CO and CO 2," *Sensors Actuators B Chem.*, vol. 238, pp. 706–715, Jan. 2017.

[45] P. Brimblecombe, *The effects of air pollution on the built environment*. 2003.

[46] R. S. Hamilton and H. Crabbe, "Environment, Pollution and Effects," in *The Effects of Air Pollution on Cultural Heritage*, 1st ed., R. Hamilton, V. Kucera, J. Tidblad, and J. Watt, Eds. Boston, MA: Springer US, 2009, pp. 1–27.

[47] J. Tidblad, V. Kucera, and S. Sherwood, "Corrosion," in *The Effects of Air Pollution on Cultural Heritage*, R. Hamilton, V. Kucera, J. Tidblad, and J. Watt, Eds. Boston, MA: Springer US, 2009, pp. 53–103.

[48] J. Watt, R. S. Hamilton, R.-A. Lefèvre, and A. Ionescu, "Soiling," in *The Effects of Air Pollution on Cultural Heritage*, Boston, MA: Springer US, 2009, pp. 105–126.

[49] D. Camuffo, "Atmospheric Water and Stone Weathering," in *Microclimate for Cultural Heritage*, Elsevier, 2014, pp. 203–243.

[50] R. A. Livingston, "Acid rain attack on outdoor sculpture in perspective," *Atmos. Environ.*, vol. 146, pp. 332–345, 2016.

[51] C. M. Grossi, P. Brimblecombe, B. Menéndez, D. Benavente, I. Harris, and M. Déqué, "Climatology of salt transitions and implications for stone weathering," *Sci. Total Environ.*, vol. 409, no. 13, pp. 2577–2585, 2011.

[52] A. Bonazza, P. Messina, C. Sabbioni, C. M. Grossi, and P. Brimblecombe, "Mapping the impact of climate change on surface recession of carbonate buildings in Europe," *Sci. Total Environ.*, vol. 407, no. 6, pp. 2039–2050, Mar. 2009.

[53] D. Sikiotis and P. Kirkitsos, "The adverse effects of nitrates on stone monuments," *Sci. Total Environ.*, vol. 171, no. 1–3, pp. 173–182, Oct. 1995.

[54] V. K. ICP Materials, "Mapping of Effects on Materials," no. August 2014, p. 10, 2004.

[55] M. Matteini, "Tecnologie per i beni culturali," Milano, 2008.

[56] P. Brimblecombe, "The composition of museum atmospheres," *Atmos. Environ. Part B. Urban Atmos.*, vol. 24, no. 1, pp. 1–8, Jan. 1990.

[57] G. Pavlogeorgatos, "Environmental parameters in museums," *Build. Environ.*, vol. 38, no. 12, pp. 1457–1462, Dec. 2003.

[58] UNI 11182:2006, "Beni culturali - Materiali lapidei naturali ed artificiali - Descrizione della forma di alterazione - Termini e definizioni." UNI, 2006.

[59] P. Brimblecombe and C. M. Grossi, "Millennium-long damage to building materials in London," *Sci. Total Environ.*, vol. 407, no. 4, pp. 1354–1361, 2009.

[60] UNI EN 15757:2013, "Conservazione dei Beni Culturali - Specifiche concernenti la temperatura e l'umidità relativa per limitare i danni meccanici causati dal clima ai materiali organici igroscopici." UNI, 2013.

[61] UNI 11130:2004, "Beni culturali - manufatti lignei - terminologia del degrado del legno." UNI, 2004.

[62] M. La Gennusa, G. Rizzo, G. Scaccianoce, and F. Nicoletti, "Control of indoor environments in heritage buildings: experimental measurements in an old Italian museum and proposal of a methodology," *J. Cult. Herit.*, vol. 6, no. 2, pp. 147–155, Apr. 2005.

[63] D. Camuffo, "Measuring Humidity," in *Microclimate for Cultural Heritage*, Elsevier, 2014, pp. 433–469.

[64] S. López-Aparicio *et al.*, "Relationship of indoor and outdoor air pollutants in a naturally ventilated historical building envelope," *Build. Environ.*, vol. 46, no. 7, pp. 1460–1468, Jul. 2011.

[65] T. Agelakopoulou, E. Metaxa, C. Karagianni, and F. Roubani-

Kalantzopoulou, "Air pollution effect of SO2 and/or aliphatic hydrocarbons on marble statues in Archaeological Museums," *J. Hazard. Mater.*, vol. 169, no. 1–3, pp. 182–189, Sep. 2009.

[66] D. Camuffo, "Environmental monitoring in four European museums," *Atmos. Environ.*, vol. 35, no. 1, pp. 127–140, 2001.

[67] M. Camaiti, S. Bugani, E. Bernardi, L. Morselli, and M. Matteini, "Effects of atmospheric NOx on biocalcarenite coated with different conservation products," *Appl. Geochemistry*, vol. 22, no. 6, pp. 1248–1254, Jun. 2007.

[68] R. Wiesinger, M. Schreiner, and C. Kleber, "Investigations of the interactions of CO2, O3 and UV light with silver surfaces by in situ IRRAS/QCM and ex situ TOF-SIMS," *Appl. Surf. Sci.*, vol. 256, no. 9, pp. 2735–2741, 2010.

[69] J. N. Crowley *et al.*, "Evaluated kinetic and photochemical data for atmospheric chemistry: Volume V – heterogeneous reactions on solid substrates," *Atmos. Chem. Phys.*, vol. 10, no. 18, pp. 9059–9223, Sep. 2010.

[70] L. G. Salmon, G. R. Cass, K. Bruckman, and J. Haber, "Ozone exposure inside museums in the historic central district of Krakow, Poland," *Atmos. Environ.*, vol. 34, no. 22, pp. 3823–3832, 2000.

[71] A. Screpanti and A. De Marco, "Corrosion on cultural heritage buildings in Italy: A role for ozone?," *Environ. Pollut.*, vol. 157, no. 5, pp. 1513–1520, May 2009.

[72] M. C. Bernard and S. Joiret, "Understanding corrosion of ancient metals for the conservation of cultural heritage," *Electrochim. Acta*, vol. 54, no. 22, pp. 5199–5205, Sep. 2009.

[73] C. Kleber, R. Wiesinger, J. Schnöller, U. Hilfrich, H. Hutter, and M. Schreiner, "Initial oxidation of silver surfaces by S2−and S4+ species," *Corros. Sci.*, vol. 50, no. 4, pp. 1112–1121, Apr. 2008.

[74] O. Unsalan and A. H. Kuzucuoglu, "Effects of hazardous pollutants on the walls of Valence Aqueduct (Istanbul) by Raman spectroscopy, SEM-EDX and Geographical Information System," *Spectrochim. Acta - Part A Mol. Biomol. Spectrosc.*, vol. 152, pp. 572–576, 2016.

[75] M. Ferm, F. De Santis, and C. Varotsos, "Nitric acid measurements in connection with corrosion studies," *Atmos. Environ.*, vol. 39, no. 35, pp. 6664–6672, 2005.

[76] D. Camuffo *et al.*, "Indoor air quality at the Correr Museum, Venice, Italy," *Sci. Total Environ.*, vol. 236, no. 1–3, pp. 135–152, 1999.

[77] K. Gysels, F. Deutsch, and R. Van Grieken, "Characterisation of particulate

matter in the Royal Museum of Fine Arts, Antwerp, Belgium," *Atmos. Environ.*, vol. 36, no. 25, pp. 4103–4113, Sep. 2002.

[78] H. Roshanaei and D. A. Braaten, "Indoor sources of airborne particulate matter in a museum and its impact on works of art," *J. Aerosol Sci.*, vol. 27, no. 96, pp. S443--S444, 1996.

[79] W. Anaf, L. Bencs, R. Van Grieken, K. Janssens, and K. De Wael, "Indoor particulate matter in four Belgian heritage sites: Case studies on the deposition of dark-colored and hygroscopic particles," *Sci. Total Environ.*, vol. 506–507, pp. 361–368, Feb. 2015.

[80] J. Grau-Bové and M. Strlič, "Fine particulate matter in indoor cultural heritage: a literature review," *Herit. Sci.*, vol. 1, no. 1, p. 8, 2013.

[81] R. S. Hamilton, D. M. Revitt, K. J. Vincent, and R. N. Butlin, "Sulphur and nitrogen particulate pollutant deposition on to building surfaces," *Sci. Total Environ.*, vol. 167, pp. 57–66, 1995.

[82] M. Ferm, J. Watt, S. O'Hanlon, F. De Santis, and C. Varotsos, "Deposition measurement of particulate matter in connection with corrosion studies," *Anal. Bioanal. Chem.*, vol. 384, no. 6, pp. 1320–1330, 2006.

[83] D. E. Searle and D. J. Mitchell, "The effect of coal and diesel particulates on the weathering loss of Portland Limestone in an urban environment," *Sci. Total Environ.*, vol. 370, no. 1, pp. 207–223, 2006.

[84] A. Li, J. Xiong, L. Yao, L. Gou, and W. Zhang, "Determination of dust and microorganism accumulation in different designs of AHU system in Shaanxi History Museum," *Build. Environ.*, vol. 104, pp. 232–242, 2016.

[85] A. Li, Z. Liu, X. Zhu, Y. Liu, and Q. Wang, "The effect of air-conditioning parameters and deposition dust on microbial growth in supply air ducts," *Energy Build.*, vol. 42, no. 4, pp. 449–454, Apr. 2010.

[86] G. Piccablotto, C. Aghemo, A. Pellegrino, P. Iacomussi, and M. Radis, "Study on Conservation Aspects Using LED Technology for Museum Lighting," *Energy Procedia*, vol. 78, pp. 1347–1352, 2015.

[87] D. Camuffo, "Radiation and Light," in *Microclimate for Cultural Heritage*, Elsevier, 2014, pp. 131–164.

[88] M. Bacci, C. Cucci, A.-L. Dupont, B. Lavédrine, M. Picollo, and S. Porcinai, "Disposable Indicators for Monitoring Lighting Conditions in Museums," *Environ. Sci. Technol.*, vol. 37, no. 24, pp. 5687–5694, Dec. 2003.

[89] UNI 10586:1997, "Documentazione. Condizioni climatiche per ambienti di conservazione di documenti grafici e caratteristiche degli alloggiamenti." 1997.

[90] UNI 10925:2001, "Beni culturali - Materiali lapidei naturali ed artificiali - Metodologia per l'irraggiamento con luce solare artificiale." UNI, 2001.

[91] C. Cacace, G. Caneva, F. Gallo, T. Georgiadas, O. Maggi, and P. Valenti, "Measurement of Environmental Physical Parameters," in *Cultural Heritage and Aerobiology*, 2003, pp. 47–79.

[92] L. Appolonia, G. Ranalli, C. Sabbioni, and C. Sorlini, "Chemical Parameters and Development of Biodeteriogens," in *Cultural Heritage and Aerobiology*, 2003, pp. 81–103.

[93] J. Grau-Bové, L. Mazzei, L. Malkii-Ephstein, D. Thickett, and M. Strlič, "Simulation of particulate matter ingress, dispersion and deposition in a historical building," *J. Cult. Herit.*, vol. 18, pp. 199–208, Mar. 2016.

[94] S. P. Corgnati, V. Fabi, and M. Filippi, "A methodology for microclimatic quality evaluation in museums: Application to a temporary exhibit," *Build. Environ.*, vol. 44, no. 6, pp. 1253–1260, 2009.

[95] D. Camuffo, "Atmospheric Stability and Pollutant Dispersion," in *Microclimate for Cultural Heritage*, Elsevier, 2014, pp. 245–282.

[96] A. W. Smyth, P. Brewick, R. Greenbaum, M. Chatzis, A. Serotta, and I. Stünkel, "Vibration Mitigation and Monitoring: A Case Study of Construction in a Museum," *J. Am. Inst. Conserv.*, vol. 55, no. 1, pp. 32–55, 2016.

[97] A. Saisi, C. Gentile, and M. Guidobaldi, "Post-earthquake continuous dynamic monitoring of the Gabbia Tower in Mantua, Italy," *Constr. Build. Mater.*, vol. 81, pp. 101–112, Apr. 2015.

[98] G. Osmancikli, Ş. Uaçk, F. N. Turan, T. Türker, and A. Bayraktar, "Investigation of restoration effects on the dynamic characteristics of the Hagia Sophia bell-tower by ambient vibration test," *Constr. Build. Mater.*, vol. 29, pp. 564–572, 2012.

[99] F. Monforti, R. Bellasio, R. Bianconi, G. Clai, and G. Zanini, "An evaluation of particle deposition fluxes to cultural heritage sites in Florence, Italy," *Sci. Total Environ.*, vol. 334–335, pp. 61–72, 2004.

[100] V. Fioriti, I. Roselli, A. Tatì, R. Romano, and G. De Canio, "Motion Magnification Analysis for structural monitoring of ancient constructions," *Measurement*, vol. 129, pp. 375–380, Dec. 2018.

[101] AA.VV, *The Effects of Air Pollution on Cultural Heritage*. Boston, MA: Springer US, 2009.

[102] D. Camuffo, "Measuring Temperature," in *Microclimate for Cultural Heritage*, Elsevier, 2014, pp. 395–432.

[103] D. Barca *et al.*, "Impact of air pollution in deterioration of carbonate building materials in Italian urban environments," *Appl. Geochemistry*, vol. 48, pp. 122–131, 2014.

[104] M. Ivaskova, P. Kotes, and M. Brodnan, "Air pollution as an important factor in construction materials deterioration in Slovak Republic," *Procedia Eng.*, vol. 108, pp. 131–138, 2015.

[105] A. Erkal, D. D'Ayala, and L. Sequeira, "Assessment of wind-driven rain impact, related surface erosion and surface strength reduction of historic building materials," *Build. Environ.*, vol. 57, pp. 336–348, 2012.

[106] R. Pucinotti, "Assessment of in situ characteristic concrete strength," *Constr. Build. Mater.*, vol. 44, pp. 63–73, Jul. 2013.

[107] D. Camuffo, A. Bernardi, G. Sturaro, and A. Valentino, "The microclimate inside the Pollaiolo and Botticelli rooms in the Uffizi Gallery, Florence," *J. Cult. Herit.*, vol. 3, no. 2, pp. 155–161, 2002.

[108] E. De Francesco and F. Leccese, "Risks analysis for already existent electric lifelines in case of seismic disaster," in *2012 11th International Conference on Environment and Electrical Engineering*, 2012, pp. 830–834.

[109] F. Leccese *et al.*, "A New Acquisition and Imaging System for Environmental Measurements: An Experience on the Italian Cultural Heritage," *Sensors*, vol. 14, no. 5, pp. 9290–9312, May 2014.

[110] A. Mecocci and A. Abrardo, "Monitoring Architectural Heritage by Wireless Sensors Networks: San Gimignano — A Case Study," *Sensors*, vol. 14, no. 1, pp. 770–778, Jan. 2014.

[111] S. Furber, *Arm system-on-chip architecture*. Pearson Education Limited, 2013.

[112] Alphasense, "Analogue Front End (AFE)," 2017. [Online]. Available: http://www.alphasense.com/WEB1213/wp-content/uploads/2015/11/AFE.pdf.

[113] Alphasense, "SO2-A4 Sulfur Dioxide Sensor," 2017. [Online]. Available: http://www.alphasense.com/WEB1213/wp-content/uploads/2013/12/SO2A4.pdf.

[114] Alphasense, "NO2-A43F Nitrogen Dioxide." .

[115] Alphasense, "NO-A4 Nitric Oxide Sensor." [Online]. Available: http://www.alphasense.com/WEB1213/wp-content/uploads/2016/03/NO-A4.pdf.

[116] Alphasense, "OX-A4 Gas Sensor Ozone," 2017. .

[117] B. Sensortec, "Combined humidity and pressure sensor." pp. 1–54, 2015.

[118] B. Sensortec, “Intelligent 9-axis absolute orientation sensor.” pp. 1–106, 2016.

[119] World Health Organization, “WHO Air quality guidelines for particulate matter, ozone, nitrogen dioxide and sulfur dioxide: global update 2005: summary of risk assessment,” *Geneva World Heal. Organ.*, pp. 1–22, 2006.

[120] UNI 9916:2004, “Criteria for the measurement of vibrations and the assessment of their effects on buildings.” 2004.

[121] UNI 10829:1999, “Beni di interesse storico e artistico - Condizioni ambientali di conservazione - Misurazione ed analisi.” 1999.

[122] R. Aguilar, E. Ramírez, V. G. Haach, and M. A. Pando, “Vibration-based nondestructive testing as a practical tool for rapid concrete quality control,” *Constr. Build. Mater.*, vol. 104, pp. 181–190, Feb. 2016.

[123] P. Pachón, V. Compán, E. Rodríguez-Mayorga, and A. Sáez, “Control of structural intervention in the area of the Roman Theatre of Cadiz (Spain) by using non-destructive techniques,” *Constr. Build. Mater.*, vol. 101, pp. 572–583, Dec. 2015.

[124] G. D’Emilia, A. Gaspari, and E. Natale, “Evaluation of aspects affecting measurement of three-axis accelerometers,” *Measurement*, vol. 77, pp. 95–104, Jan. 2016.

[125] M.-G. Masciotta, J. C. A. Roque, L. F. Ramos, and P. B. Lourenço, “A multidisciplinary approach to assess the health state of heritage structures: The case study of the Church of Monastery of Jerónimos in Lisbon,” *Constr. Build. Mater.*, vol. 116, pp. 169–187, Jul. 2016.

[126] L.-R. ARPA, “Rapporti Giornalieri - Comune di Roma,” *Rapporti Giornalieri - QUALITA’ ARIA*, 2017. [Online]. Available: http://www.arpalazio.net/main/aria/sci/basedati/rpgg.php?prov=RMC. [Accessed: 15-Feb-2017].

[127] A. Tittarelli *et al.*, “Estimation of particle mass concentration in ambient air using a particle counter,” *Atmos. Environ.*, vol. 42, no. 36, pp. 8543–8548, Nov. 2008.

[128] F. Leccese, M. Cagnetti, S. Tuti, P. Gabriele, R. De Francesco, Edoardo Đurović-Pejčev, and A. Pecora, “Modified LEACH for Necropolis Scenario,” in *IMEKO International Conference on Metrology for Archaeology and Cultural Heritage, Lecce, Italy, October 23-25, 2017*, 2017.

[129] M. Jovašević-Stojanović, A. Bartonova, D. Topalović, I. Lazović, B. Pokrić, and Z. Ristovski, “On the use of small and cheaper sensors and devices for indicative citizen-based monitoring of respirable particulate matter.,”

Environ. Pollut., vol. 206, pp. 696–704, Nov. 2015.

[130] ISO IEC 31010:2009, "Risk management – Risk assessment techniques Gestion," 2010.

[131] M. Andretta, F. Coppola, A. Modelli, N. Santopuoli, and L. Seccia, "Proposal for a new environmental risk assessment methodology in cultural heritage protection," *J. Cult. Herit.*, vol. 23, pp. 22–32, 2016.

[132] L. D'Alvia, E. Palermo, S. Rossi, and Z. Del Prete, "Validation of a low-cost wireless sensors node for museum environmental monitoring," *ACTA IMEKO*, vol. 6, no. 3, p. 45, Sep. 2017.

[133] L. D'Alvia, E. Palermo, and Z. Del Prete, "Validation and application of a novel solution for environmental monitoring: A three months study at 'Minerva Medica' archaeological site in Rome," *Measurement*, vol. 129, no. July, pp. 31–36, Dec. 2018.

[134] ISO 37120:2014, "Sustainable development of communities — Indicators for city services and quality of life," 2014. [Online]. Available: https://www.iso.org/obp/ui/#iso:std:iso:37120:ed-1:v1:en. [Accessed: 15-Sep-2017].

[135] F. W. Lipfert, "Atmospheric damage to calcareous stones: Comparison and reconciliation of recent experimental findings," *Atmos. Environ.*, vol. 23, no. 2, pp. 415–429, Jan. 1989.

[136] T. Grøntoft and M. R. Raychaudhuri, "Compilation of tables of surface deposition velocities for O3, NO2 and SO2 to a range of indoor surfaces," *Atmos. Environ.*, vol. 38, no. 4, pp. 533–544, 2004.

[137] V. Kucera and J. Tidblad, "Model for multi-pollutant impact and assessment of threshold levels for cultural heritage," Stockholm, 2005.

[138] N. Ghedini, I. Ozga, A. Bonazza, M. Dilillo, H. Cachier, and C. Sabbioni, "Atmospheric aerosol monitoring as a strategy for the preventive conservation of urban monumental heritage: The Florence Baptistery," *Atmos. Environ.*, vol. 45, no. 33, pp. 5979–5987, Oct. 2011.

[139] T. Q. Thach, H. Tsang, P. Cao, and L. M. Ho, "A novel method to construct an air quality index based on air pollution profiles," *Int. J. Hyg. Environ. Health*, vol. 221, no. 1, pp. 17–26, Jan. 2018.

[140] G. Forino, J. MacKee, and J. von Meding, "A proposed assessment index for climate change-related risk for cultural heritage protection in Newcastle (Australia)," *Int. J. Disaster Risk Reduct.*, vol. 19, pp. 235–248, 2016.

[141] X. Romão, E. Paupério, and N. Pereira, "A framework for the simplified risk analysis of cultural heritage assets," *J. Cult. Herit.*, vol. 20, pp. 696–708,

2016.

[142] T. Aven, "On how to define, understand and describe risk," *Reliab. Eng. Syst. Saf.*, vol. 95, no. 6, pp. 623–631, 2010.

[143] M. Andretta, "Some Considerations on the Definition of Risk Based on Concepts of Systems Theory and Probability," *Risk Anal.*, vol. 34, no. 7, pp. 1184–1195, 2014.

[144] UNI ISO 31000:2010, "Gestione del rischio Principi e linee guida," 2010.

[145] L. D'alvia, E. Palermo, and Z. Del Prete, "Application of a novel monitoring technology at ' Minerva Medica Temple ' archaeological site in Rome," in *IMEKO International Conference on Metrology for Archaeology and Cultural Heritage, Lecce, Italy, October 23-25*, 2017.

Academic Results

CONFERENCE

[1] 4th IEEE International Conference on Metrology for Archaeology and Cultural Heritage, Cassino, Italy, October 22-24, 2018. (Session Chair of SS1; 2 posters, 1 oral).

[2] 2nd Forum Nazionale delle Misure, Padova, Italy, September 17-19, 2018. (1 poster).

[3] 7th Cycle Ph.D. School "Italo Gorini", CERN-Geneva, Switzerland, September 10-14, 2018.

[4] 13th IEEE International Symposium on Medical Measurements and Applications, Rome, Italy, June 11-13, 2018. (1 poster).

[5] 3rd IMEKO International Conference on Metrology for Archaeology and Cultural Heritage, Lecce, Italy, October 23-25, 2017. (1 oral)

[6] 1st Forum Nazionale delle Misure, Modena, Italy, September 13-16, 2017.

[7] International Summer School "ENVIMAT", Budapest, Hungary, June 27-29, 2017. (1 poster).

[8] 2nd IMEKO International Conference on Metrology for Archaeology and Cultural Heritage, Torino, Italy, October 19-21, 2016. (1 oral).

AWARDS

Grant "Avvio alla ricercar 2016": Sistema a basso costo per la valutazione del "Comfort di Beni Culturali in ambiente indoor" mediante wireless sensor network. **Funding:** EUR 1000 • Sapienza University • "Research Starts" **Principal Investigator:** Livio D'Alvia • **Co-investigators:** Paolo Cappa

PAPERS AD PROCEEDINGS

[1] L. D'Alvia and Z. Del Prete, "WENDY: A Wireless Environmental Monitoring Device Prototype", in 4th IEEE International Conference on Metrology for Archaeology and Cultural Heritage, Cassino, Italy, October 22-24, 2018, pp. 0–3.

[2] L. D'Alvia et al., "Effect of Applied Pressure on Patch ResonatorBased Measurements of Moisture Level for Cultural Heritage Materials", in 4th IEEE International Conference on Metrology for Archaeology and Cultural Heritage, Cassino, Italy, October 22-24, 2018, pp. 20–22.

[3] E. Piuzzi et al., "Compensating for Bulk Density Effect in Permittivity-Based Moisture Content Measurements on Cultural Heritage Materials", in 4th IEEE International Conference on Metrology for Archaeology and Cultural Heritage, Cassino, Italy, October 22-24, 2018.

[4] S. Parisi et al., "Il ruolo della gait-analisys nella valutazione del 6MWT in pazienti affetti da sclerosi sistemica: studio preliminare", in 55th Congresso Nazionale della Società Italiana di Reumatologia, Nov. 21-24, 2018

[5] L. D'Alvia et al., "Validation and application of a novel solution for environmental monitoring: A three months study at 'Minerva Medica' archaeological site in Rome," Measurement, vol. 129, pp. 31–36, Dec. 2018.

[6] F. Mangini et al., "Tag recognition: a new methodology for the structural monitoring of cultural heritage", Measurement, vol. 127, pp. 308–313, Oct. 2018.

[7] L. D'Alvia et al., "Tetrapolar Low-Cost Systems for Thoracic Impedance Plethysmography", in 14th IEEE International Symposium on Medical Measurements and Applications, 2018.

[8] L. Apa et al., "Development and mechanical validation of an in vitro system for bone cell vibration loading", in 14th IEEE International Symposium on Medical Measurements and Applications, 2018.

[9] L. D'Alvia et al., "Validation of a low-cost wireless sensors node for museum environmental monitoring", ACTA IMEKO, vol. 6, no. 3, p. 45, Sep. 2017.

[10] L. D'alvia, et al., "Application of a novel monitoring technology at 'Minerva Medica Temple' archaeological site in Rome", in 3rd IMEKO International Conference on Metrology for Archaeology and Cultural Heritage, Lecce, Italy, October 23-25, 2017.

[11] L. D'Alvia, E. Palermo, S. Rossi, and P. Cappa, "Development of wireless sensor network for museum environmental monitoring", in 2nd IMEKO International Conference on Metrology for Archeology and Cultural Heritage, Torino, Italy, October 19-21, 2016, 2016.

Acknowledgements

Quando ti trovi a scrivere per la terza volta i ringraziamenti alla fine di una tesi pensi di avare ormai scritto e ringraziato tutti nelle puntate precendenti. Invece soffermandoti a pensare a come sia cambiata la propria vita in questi anni, ecco che si realizza come, invece, esista ancora una volta quella piacevole, sincera e doverosa volgia di dire GRAZIE.

Questa tesi e questo percorso sono stati figli di un periodo che definere a luci e ombre è poco ma che al tempo stesso mi hanno fatto consocere un mondo nuovo e persone meravoglise che definire amici è poco: la famiglia del "GRS allargato". Dove il "MarcoMarco21212121!!!!!", il "Filippo zitto che sto parlado con Filippo", "Passami il.. Ricciotto", "Maria tirami il dito e le corse sul 23 erano il nostro pane quotidiano. Grazie di vero cuore a tutti voi.

Anche qui definirla famiglia è poco, considerando da quanti anni ci si conosce e sebbene negli ultimi tempi, purtoppo per via di età e esigenze diverse, ci si è un po' allontanti, siete e restate parte di me.

Un grazie va al Prof. Paolo Cappa, per aver creduto in me sebbene non mi conoscese, e a tutto il PK-team. Ma dove si poteva trovare prof. più figo, che giocando sulle proprie inazili aveva l'mmagine di Paperinik su skype?? Grazie a tutti – Andrea, Eduardo, Emanuele, Emila, Francesca, Ilaria, Juri, Ludovica, Stefano e Roberto – per avermi accolto nel laboratorio e nel vostro gruppo, e sebbene io sia caratterialemente come un'orso in letargo c'è chi non ha mollato un giorno pur di farmi parlare (…Emilia…).

Un secondo grazie, ma altrettanto importante, è per il Prof. Zaccaria Del Prete (per noi Zac.. per tutti gli altri Rino), che quel maledetto 28 agosto ha voluto credere in tutti noi e ci ha accompagnato fino alla fine di questo viaggio. Grazie.

Per finire un grazie va alla mia famiglia allargata, che ha avuto la pazienza di accettare questo percorso (sia il mio che di Ilaria) così lontano dal loro ma che rappresenta tutto per noi.

E poi c'è lei, ♡Ilaria♡, che è entrata nella mia vita e nel mio cuore sei anni fa, là dove caso e distino si intrecciano. Dirle GRAZIE è poco e le parole non basterebbero. Ora inizia, per entrambi, un nuovo percorso insieme, che chissà dove ci portorà.. o forse sì?